論文 / 著書情報
Article / Book Information

題目(和文)	ヒトデ卵における極体放出の制御
Title(English)	Regulation of polar body emission in starfish oocytes
著者(和文)	HASANUCAR
Author(English)	hasan ucar
出典(和文)	学位:博士(理学), 学位授与機関:東京工業大学, 報告番号:甲第9356号, 授与年月日:2013年12月31日, 学位の種別:課程博士, 審査員:立花 和則,徳永 万喜洋,伊藤 武彦,山口 雄輝,田中 幹子,相澤 康則
Citation(English)	Degree:Doctor (Science), Conferring organization: Tokyo Institute of Technology, Report number:甲第9356号, Conferred date:2013/12/31, Degree Type:Course doctor, Examiner:,,,,,
学位種別(和文)	博士論文
Type(English)	Doctoral Thesis

PhD Thesis

2013

Regulation of polar body emission in starfish oocytes

Hasan UCAR

Tokyo Institute of Technology

Department of Biological Information

Graduate School of Bioscience and Biotechnology

Advisors:

Associate Prof. Kazunori Tachibana

(Previous: Prof. Takeo Kishimoto)

TABLE OF CONTENTS **Page**

1. ABBREVIATIONS

1-MeAde	: 1-methyladenine
APC/C	: Anaphase promoting complex/ cyclosome
ApDia	: *Asterina pectinifera* Diaphanous-related formin
Arp2/3 complex	: Actin related protein 2/3 complex
Cdc	: Cell division cycle
CDK	: Cyclin-dependent kinase
DAD	: Diaphanous autoregulatory domain
DID	: DAD interacting domain
Erp1/Emi2	: Emi1 related protein 1/ Early mitotic inhibitor 2
GBD	: GTPase binding domain
GV	: Germinal vesicle
GVBD	: Germinal vesicle breakdown
MAPK	: Mitogen-activated kinase
MCM	: Minichromosome maintenance
MEK	: MAPK/extracellular signal-regulated kinase kinase
MosAS	: Mos antisense oligonucleotide
p90Rsk	: p90 ribosomal S6 kinase
pre-RC	: Pre-replicative complex
PBE	: Polar body emission
PDK	: Phosphoinositide-dependent kinase
RhoA	: Ras homology member A
RhoGAP	: Rho-GTPase activating factor
RhoGEF	: Rho-guanidine exchange factor
SMIFH2	: Small molecule inhibitor of FH2

2. SUMMARY

The haploid female gametes are produced by extruding half of the genetic material into polar bodies which removes very little cytoplasm (polar body emission, PBE), thus the oocyte saves much of the cytoplasm to support itself for the early embryonic development after fertilization. During PBE, the spindle is positioned under the oocyte cortex. Then, one spindle pole and half of chromosomes are extruded into a membrane protrusion, after which the cleavage furrow forms and closes at the neck of the protrusion.

The Mos-MAPK-p90Rsk pathway is a meiosis specific cell cycle regulatory pathway. It is required for transition from meiosis-I to meiosis-II, and for the secondary meiotic arrest (G1 arrest in starfish oocytes). Several studies suggest that the Mos-MAPK pathway is required for PBE; however its role during PBE remains unclear.

In this study, first of all, I have concentrated on whether the Mos-MAPK pathway is required for PBE in starfish oocytes or not. For this purpose, immature oocytes were injected with antisense oligonucleotide against Mos (MosAS) to prevent Mos synthesis or treated with a MEK-specific inhibitor, U0126, to prevent MAPK activity. To visualize spindle and chromosome dynamics in these oocytes, immature oocytes were injected with fluorescent labeled histone and tubulin proteins, and then the maturing oocytes were observed with live-cell imaging. In contrary to control oocytes, MosAS injected oocytes or MAPK-inhibited oocytes failed in PBE; in these oocytes the spindles were not kept tightly attached to the cortex, chromosomes were not segregated properly, and finally, although a membrane protrusion for a polar body was formed, the cleavage furrow failed to close. Next, immature oocytes

were injected with a constitutively active mutant of p90Rsk (CA-p90Rsk) or a kinase dead mutant (KD-p90Rsk), and treated with U0126. CA-p90Rsk was able to recover all the defects caused by U0126-treatment while KD-p90Rsk was not. This latter observation, suggests that p90Rsk might be performing the functions of MAPK during PBE. Thus, I have shown that the Mos-MAPK-p90Rsk pathway is required for PBE in starfish oocytes.

Since there was a defect in cleavage furrow closure, I have concentrated on the regulation of the F-actin mechanisms to find a downstream target of the Mos-MAPK-p90Rsk pathway. Diaphanous-related formins (Dia) are actin nucleating factors that are known to be required for contractile ring formation at the cleavage furrow during mitotic division and during budding of the yeast. Treatment of oocytes with a formin specific inhibitor, SMIFH2, prevented cleavage furrow closure during PBE. Based on this, *Asterina pectinifera* Dia (ApDia) was cloned, and then the oocytes expressing GFP2-ApDia was monitored during PBE; GFP2-ApDia had a ring like localization at the neck of the protrusion, and its localization was altered in MAPK-inactivated oocytes. To analyze whether activity of ApDia was also under the control of MAPK, in the absence of MAPK activity, endogenous ApDia was activated by injecting the immature oocytes with GST-DAD (GST-Dia autoregulatory domain) or GST-GBD/DID (GST-GTPase binding domain/DAD interacting domain) peptide fragments, and this activation recovered all defects caused by U0126-treatment. Finally, expressing a constitutively active form of ApDia (ApDia-fsDAD) rescued PBE in the absence of MAPK-activity whereas an actin binding mutant (ApDia-fsDAD-I699A) did not.

To sum up, I have shown in this study that, the Mos-MAPK-p90Rsk pathway is required for PBE by maintaining tight spindle attachment, proper chromosome separation and cleavage furrow closure. I have also shown that localization of ApDia to cleavage furrow and its activation is being regulated by the activity of the Mos-MAPK pathway. My results suggest that Dia activity downstream of MAPK is required for cleavage furrow closure during PBE.

3. INTRODUCTION

3.1 Equal cell division and unequal cell division

In most of the somatic cells, equal cell division takes place after which two daughter cells have the same morphology with same cell sizes and shapes, and same physiology with same amount of membrane, cytoplasmic and nuclear components of lipids, proteins and mRNA (Field and Oegema, 1999). To establish same morphology in equal cell division, during metaphase, the mitotic spindle forms at the center of the mother cell, long astral microtubules are symmetrically aligned at both ends, which help central localization of the spindle, and the chromosomes are aligned at the metaphase plate at the center of the spindle (Field and Oegema, 1999; Compton, 2000). Upon anaphase start, chromosomes are separated and cleavage furrow formation starts at the cell membrane at around the metaphase plane with a symmetric membrane organization in both sides of the plate (Schiel and Prekeris, 2013). In the formation of the cleavage furrow an actin dependent contractile ring is involved, and the cleavage furrow starts closing by the aid of the non-muscle Myosin-II activity in the contractile ring at the time when the chromosomes move apart from each other. The actomyosin contraction causes an ingression at the cell membrane and this stage is the starting point for cytokinesis. During telophase, ingression at the membrane continues in between separated chromosomes due to actomyosin contraction (Lee et al., 2012). The closing cleavage furrow forms the mid-body structure, an electron-dense protein rich material in a very restricted area, between the daughter cells. Upon completion of abscission of cellular membrane between cells, cytokinesis is completed resulting in two symmetric daughter cells with equal cell sizes and equal

cellular components (Barr and Gruneberg, 2007; Fededa and Gerlich, 2012) (Fig. 3-1).

On the other hand, many cells perform unequal cell division in which the resulting daughter cells might be different in their size, shape and cytoplasmic and membrane components (Horvitz and Herskowitz, 1992). Accordingly with their differences, these daughter cells have different cell fates. Examples of unequal cell division could be encountered in many cell types in adult body (stem cells like neuroblasts, erythrobloasts etc), during early or late developmental stages (early cleavage cycles after the loss of totipotency or during the tissue differentiations), and during gamete production of female organisms (Hawkins and Garriga, 1998; Kaltschmidt and Brand, 2002). The latter one will be under consideration in this study as polar body emission (PBE) during oocyte maturation of starfish oocytes.

One of the main points in unequal cell division, which causes difference in daughter cell sizes, is that during metaphase, mitotic spindle is not localized at the center of the mother cell; instead, the spindle might be formed slightly eccentrically or even under the cell membrane which results in a polarized architecture of the mother cell (Fig. 3-1). Accordingly, lengths of the astral microtubules are different in the opposite sides of spindle when the spindle is eccentrically positioned (Kaltschmidt and Brand, 2002). This difference in astral microtubule length might be functioning together with actin cytoskeleton to determine the eccentric localization of the spindle. When spindle is formed under the membrane (during oocyte maturation), the length of astral microtubules becomes very short in both ends indicating that they cannot function in the regulation of spindle localization, and thus, actin

cytoskeleton might be the main regulator of the spindle localization in this case (McNally, 2013).

In parallel with the localization of eccentric spindle localization, membrane organization of the mother cell also shows a polarized architecture. One of the most studied families of the proteins showing polarized organization is the PAR protein family which initially found to be important in determination of the anterior and posterior poles in the zygote in *C.elegans* embryo (Nance, 2005). These proteins were later shown to be important in polarity determination in other unequal cell division systems (Vinot et al., 2004; Duncan et al., 2005). In addition, small GTPases are also distributed asymmetrically on the cell membrane in oocytes causing differential cortical actin and myosin organizations at the animal poles and vegetal pole (see F-actin regulation during PBE). Similar to protein organizations, lipid components of membrane regions are also differentially regulated during unequal cell divisions (Lu and Johnston, 2013).

3.2 Cell division cycle

3.2.1 General review of mitotic cell division cycle

A somatic cell first grows, duplicates its genetic material and then divides into two, and then grows again generating so called `cell division cycle` in which there are several steps and regulations. The cell division cycle is composed of interphase, in which cells grow, duplicate its genomic DNA and prepare for the cell division and M-phase (mitosis), in which cell division occurs. During interphase, there are 3 steps; G1 (Gap-1), S (Synthesis) and G2 (Gap-2) phases. Thus a cell division cycle is typically a successive and continuous cycle of G1-S-G2-M phases and cytokinesis (Murray and Hunt, 1993; Nurse, 1994). (Fig. 3-2)

Generally, G1 of the interphase is the longest phase in a cell division cycle and cells have time for growth (Cooper, 1979; Pardee, 1989). During this time, new proteins or lipids are produced, or any damages in the cell body are repaired (Hartwell and Weinert, 1989; Pardee, 1989). In some cases, like muscle cells and neurons, cells enter G0 phase in which they cease their cell division cycle, differentiate and survive for long times without cell division (Pardee, 1989; Zetterberg et al., 1995). In actively proliferating cells, successive to G1, doubling of the genetic material (DNA replication) and the centrosome take place in the S-phase (Laskey et al., 1989; Doxsey, 2001). After S-phase, in the other gap phase (G2) cells check and repair any damages that might have occurred during the DNA synthesis. If the cell has accomplished the DNA synthesis without errors then it is committed to enter the M-phase(Hartwell and Weinert, 1989; Murray, 1994).

M-phase is also composed of sub-phases that are prophase, metaphase, anaphase and telophase (Mitchison and Salmon, 2001; Paweletz, 2001; De Souza and Osmani, 2007). During prophase nucleolus disappears, chromatin are packed into chromosomes, duplicated centrosomes are separated, and the nuclear envelope breakdown (NEBD) takes place. Since the DNA was duplicated during S-phase there are 2 copies of each chromosomes (sister chromosomes) which are facing each other and connected strongly at a region called centromere (Comings and Riggs, 1971). Unlike chromosomes, the duplicated centrosomes are pushed apart from each other by the effect of microtubule nucleation while keeping bridges of microtubule fibers in between. During metaphase, the condensed sister chromosome pairs are found and attached by microtubules at their kinetochores from both sides of sister chromosomes, and then aligned at the metaphase plate (equatorial plate) which is an imaginary line at an equal distance between two centrosomes. At this stage each sister chromosome is attached and counterpoised by microtubule fibers from opposite centrosomes, forming the mitotic spindle (Cheeseman and Desai, 2008). Upon the completion of chromosome alignment anaphase starts in which chromosomes are pulled and pushed apart from each other at their kinetochores by the effect of microtubules. Simultaneous with this, the non-kinetochore microtubules slide on each other and cause the continuous separation of centrosomes poles from each other. During telophase, now chromosomes are apart, and while cytokinesis is being completed the events of prophase are to be reversed; two nuclear envelopes are formed while chromosomes de-condense into

chromatin, nucleoli are formed and the microtubule fibers disintegrate (Weiss, 2012).

3.2.2 Regulation of mitotic cell cycle

Cell division cycle is regulated by several protein interactions which of the most important ones are cyclin and cyclin-dependent kinases (Cdk). Cyclins are a family of proteins which show cycling expression patterns that are parallel with the cell division cycle. And Cdks are Ser/Thr kinases that are active only when they are in complex with a cyclin protein (Murray and Hunt, 1993; Malumbers and Barbacid, 2005).

Cdk proteins are constitutively expressed through the cell cycle but different cyclins are produced at different phases of cell cycle, which enables different cyclin-cdk pairs to function in different phases. CycD-Cdk6 and CycD-Cdk4 together with CycE-Cdk2 are required for the transition from G1-phase to S-phase by regulating gene expression switches. CycE-Cdk2 functions in early S-phase also. In S-phase, CycE-Cdk2 and CycA-Cdk2 is required for the regulation of DNA replication initiation together with another cell cycle regulator, DDK (Dbf4 dependent kinase; Cdc7-Dbf4 complex). Cdk and DDK activities are required for the transition from pre-replication complex to pre-initiation complex, and thus for the start of the DNA replication (Nigg, 1995; Pines, 1999; Lei and Tye, 2001). (Fig. 3-2)

After the completion of S-phase, CycA-Cdk complex persists until the the M-phase Cdk-complex, the CycB-Cdk1, accumulates (Dorée and Hunt, 2002). CycB synthesis starts before M-phase, and Thr161 at Cdk1 is phosphorylated by CAK (Cdk-activating kinase) upon CycB-Cdk1 complex formation, but Wee1 and Myt1 activities keep the CycB-Cdk1 complex inactive by phosphorylating Thr14 and Tyr15 residues of Cdk1. At the onset of M-phase, to activate CycB-Cdk complex, these inhibitory phosphates are removed by a

phosphatase (Cdc25) (Fisher et al., 2012). CycB-Cdk1 activity is required for several steps to promote metaphase. CycB-Cdk1; 1) promotes chromosome condensation by phosphorylating condensin and histone proteins (Tadani et al., 2012), 2) causes NEBD by phosphorylating lamins in the nuclear lamina (Fields and Thompson, 1995), 3) triggers and maintains spindle formation by phosphorylating various microtubule-associated proteins (John et al., 2001). And to keep the cells in metaphase, CycB-Cdk1 phosphorylates securin proteins which in turn bind to and inhibit separase. Active separase cleaves the cohesin proteins which hold the sister chromatids together. Moreover, CycB-Cdk1 also prevents myosin-II activity which prevents constriction at the cleavage furrow and start of cytokinesis (Matsumura et al., 2011; John et al., 2001). During M-phase, polo-like kinase-1 (Plk1) is also important in several steps. Firstly, downstream of CycB-Cdk1, Plk1 is required for the positive feedback loop of CycB-Cdk1 activation by changing the balance of Myt1/Wee1 and Cdc25 activities, and secondly, Plk1 is also important for centrosome maturation and bipolar spindle formation (Nigg, 1998).

At the start of anaphase, anaphase-promoting complex/cyclosome (APC/C), which is an E3-ubiquitin ligase, is activated by Plk1 and then APC/C promotes exit from mitosis (Eckerdt and Strebhardt, 2006; Cohen-Fix and Koshland, 1997). CycB is poly-ubiquitinated near its destruction box at the N-terminus by APC/C, and the CycB is degraded proteasome dependently (Peters, 2006). APC/C also targets securin proteins for degradation and relieves separase. Consequently, the activated separase, which is a protease, cleaves cohesins and induces chromosome separation (Peters, 2006; Vodermaier 2004; Nasmyth, 2005). Activity of Plk1 at anaphase drives

cleavage furrow formation by mediating cortical reorganization around the equatorial plate (Petronczki et al., 2008; Barr and Gruneberg, 2007) (please see roles of actin-mechanisms in cell division).

3.2.3 Meiotic cell cycle

In sexually reproducing organisms, male and female gametes are fused to form the zygote which then produces the new organism by successive mitotic divisions. But, to maintain the amount of genetic material constant in new generations, the gametes should be haploid (have single copies of each chromosome; n), having half amount of genetic materials that of the reproducing diploid (having two copies of each chromosome; 2n) organisms. Reducing of the genetic material from diploid to haploid is accomplished by meiotic cell division during gametogenesis, in which sperms and oocytes are produced from gametogonia in gonads (Rasmussen and Holm, 1980).

The mechanisms involved in meiotic division are similar with mitotic division but there are some very essential differences. Most importantly, although the division cycle starts with an S phase and the chromosomes are duplicated; two successive M-phases (meiosis-I and meiosis-II) take place without an intervening S-phase resulting in 4 haploid daughter cells. Secondly, in meiosis, chromosome recombination (crossover) in which genetic material shuffling between homologous chromosomes (the pair of chromosomes one originating from mother, the other form father) can take place (Riley and Flavell, 1977; Phadnis et al., 2011).

After the S phase, meiosis-I starts which has similar steps with the steps of M-phase of mitosis; prophase-I, metaphase-I, anaphase-I and telophase-I. Most of the mechanisms during these phases are similar with that of mitosis, but in prophase-I, the chromosomes are aligned different from that of mitosis; homologous chromosomes are paired with synoptonemal complexes forming the bivalents (that are tetrads of chromatids). In this

alignment, chromatids of one homolog chromosome are closely attached with chromatids of other homolog chromosome (Maquire, 1990). During this pairing, chromosomal recombination occurs; some gene segments are exchanged between chromatids at the regions called chiasmata by physical breaking and ligating, which results in the formation crossing over (Cromie and Smith, 2007). Chiasmata physically support the pairing of homologous chromosomes because it involves packing of chromosome arms by the cohesin complex. Each of the homolog chromosomes of the bivalent is attached to the microtubule fibers emerging from opposite centrosomes. This alignment causes the separation of homologous chromosomes during anaphase instead of sister chromatids so that the chromosome amount is halved (Yanowitz, 2010).

After the completion of meiosis-I, the cytokinesis is completed, and then without an S phase or any interphase step, meiosis-II starts which has the steps homologous to mitosis (Yanowitz, 2010). (Fig. 3-3)

3.2.4 Oocyte maturation

Although both sperms and oocytes are produced with the same mechanisms of meiotic cell division, different from sperm formation, oocytes are produced by a highly specialized form of unequal cell division and the maturation of oocytes has some additional regulations (Evans and Robinson, 2011). All animals have their oocytes grown in their gonads and have them arrested in their prophase stage of meiosis-I. This is called the first meiotic arrest or prophase-I arrest. During this stage the oocytes get fully grown and accumulate the necessary components to start metaphase-I (Maller, 1985). Upon stimulation with a maturation inducing hormone oocytes are released from prophase-I arrest, which is equivalent to G2/M-phase transition of somatic cells (Kishimoto, 1998; Kishimoto, 2003), and oocyte maturation takes pace in which oocytes get ready for fertilization and zygote formation. In physiological conditions the hormone originates from the cells around the oocyte, but the oocyte maturation can be initiated *in vitro* by the addition of the hormone into the oocyte medium.

Oocyte maturation is hallmarked by GVBD (germinal vesicle breakdown), PBE (polar body emission) and the second meiotic arrest. The second meiotic arrest is a phase when oocytes await fertilization. The second meiotic arrest takes place at different stages in different organisms; echinoderm (includes starfish) oocytes and cnidarian oocytes are arrested at G1 phase after completion of meiosis-II, vertebrate oocytes are arrested at metaphase-II, and insect, mollusk and ascidian oocytes are arrested at metaphase-I (Masui and Markert, 1971; Sagata, 1996; Kishimoto, 2003).

3.2.4.1 Oocyte maturation in starfish

In oocytes arrested at prophase-I (immature oocytes), CycB-Cdk1 complex is already formed but it is kept in its inactive form (phosphorylated at Thr14 and Tyr15 of Cdk1). In starfish oocytes, upon hormonal stimulus with 1-methyladenine (1-MeAde), which is the first maturation-inducing hormone identified in the animal kingdom (Kanatani et al., 1969), MPF activity, which is attributed to CycB-Cdk1 and Greatwall kinase activities, is triggered by a cascade of enzymatic events. The hormonal stimulus activates protein kinase B/Akt in a PIP3, PDK1 and PDK2/TORC2-dependent mechanism on the cell surface, and then Akt down-regulates Myt1 activity while up-regulating Cdc25 activity which are key regulators for the phosphorylation status of Thr14 and Tyr15 of Cdk1. By doing so, Akt triggers activation of CycB-Cdk1 by changing the activity balance between Cdc25 and Myt1 activities towards Cdc25 activity. Activated CycB-Cdk1 then promotes synthesis of Mos and activation of other kinases that are required both for positive feedback loop for CycB-Cdk1 activity and meiotic maturation; Plk1, Aurora, Greatwall kinase. Upon induction of MPF activity, GVBD, which is the hallmark of M-phase entry, takes place. After GVBD, PBE which is an extreme example of unequal cell division (see `polar body emission`) takes place two times successively which are hallmarks of completion of meiosis-I and meiosis-II. Plk1 and Aurora are major kinases for the accomplishment of meiotic divisions as they are for the mitotic divisions (Taylor and Peters, 2008). After completion of meiosis-II, starfish oocytes are arrested at G1 phase which is the second meiotic arrest in echinoderms (Fig. 3-4). The second meiotic arrest in starfish and other animals that are studied (regardless of at which step the arrest takes place) is maintained by the

continuous synthesis of Mos protein which activates the downstream kinases MAPK (mitogen activated kinase) and p90Rsk (90 kDa ribosomal S6 kinase). The Mos-MAPK-p90Rsk pathway is also important for prevention of parthenogenesis after completion of meiosis-I (see `Mos-MAPK-p90Rsk pathway in oocyte maturation`). But the involvement of the Mos-MAPK-p90Rsk pathway in PBE in starfish oocytes was not studied until the current study of mine.

3.2.5 Polar body emission

Polar body emission (PBE) is an extreme example of unequal cell division. At metaphase, the spindle is located under the oocyte cortex and its long axis is perpendicular to the cell surface. Due to this localization, metaphase plate is not at the center of the cell but at animal pole just under the cortex. Thus, cell divisions of meiotic cell cycle results in a big oocyte and small cell bodies that are called polar bodies (PB). This pattern of division is to reduce the chromosome number by extruding chromosomes into the PB which removes only a very small portion of the cytoplasm (~0.1 % in starfish oocytes) and to retain most of the cytoplasm in the oocyte. The oocyte will be fertilized and constitute the new organism and retained cytoplasmic content will be used during the early cleavage cycles (McCarthy and Goldstein, 2006).

The prophase-I arrested oocytes have a big GV either at the center of the oocyte (mammals) or close to the animal pole of the oocyte (most of other organisms including starfish, cnidarians and amphibians) (Liu et al., 2012). In these immature oocytes chromosomes are not condensed yet, and then upon maturation induction, the chromosomes are condensed. After GVBD, microtubule fibers form and capture the condensed chromosomes, and then the meiotic spindle is formed inside the GV area. In mammals, since the GV in the immature oocytes is at the center of the oocyte, the spindle must be moved to the animal pole and then attached to the oocyte cortex (Liu et al., 2012). Since meiotic spindles have very short astral microtubule fibers, it is plausible to think that astral microtubules cannot contribute to the localization of spindle inside the oocyte (McNally, 2013). Consistently, in mouse oocyte, which is well studied for the control of spindle localization, the spindle movement is shown

to be dependent on the dynamics of filamentous actin (F-actin) (Dumont et al., 2007; Pfender et al., 2011). In mouse oocytes cortical polarity is not predetermined and the spindle is moved to the closest cortex along its long axis and reaches to the cortex perpendicularly (Azoury et al., 2009). On the other hand, in other organisms that have their GV near the animal pole, spindle is formed underneath the cortex, thus spindle movement might be less prominent. In this case spindle must be attached at one of its poles and then must be rotated so that it is perpendicular to the surface (Fig. 3-5). Like spindle movement, spindle rotation is also mediated by F-actin dynamics (Gard, 1992; Zhang et al., 2008).

Spindle localization under the oocyte cortex maintains the equatorial plate to be placed asymmetrically, that is under the animal pole cortex. The polar body is emitted as a protrusion, containing half of the genetic material, and then the contractile ring is formed at the neck of the protrusion in between separated chromosomes (Liu et al., 2012). During PBE, fine localization of branched and straight F- actin and formation of the contractile ring are tightly regulated (see `F-actin regulation during PBE`). This pattern of division maintains most of the cytoplasm in the oocyte while discarding half of the genetic material with a negligible amount of cytoplasm into the PB (McCarthy and Goldstein, 2006) (Fig. 3-5).

3.3 Actin regulation and its role in cell division

3.3.1 Regulators of F-Actin Nucleation

Actin is a 42kDa ATP binding globular protein (G-actin) which can be polymerized into filamentous actin (F-actin) and form one of the most fundamental cytoskeletal elements of cells. Actin can have a spontaneous cycle of self-assembly of actin-dimers and actin-trimers, ATP hydrolysis and depolymerization. But to construct stable and long F-actin, additional nucleation and elongation factors are necessary. F-actin has barbed end at where actin nucleation and depolymerization dynamics are high and pointed end at where F-actin is more stable. There are 3 classes of F-actin nucleators; Arp2/3 complex, formin family and WH2-domain containing nucleators. Arp2/3 complex produces branched F-actin while formin and WH2-domain containing nucleators produce straight F-actin (Chesarone et al., 2010; Campellone and Welch., 2010).

Arp2/3 complex is the unique actin nucleator that can produce branched F-actin. The complex is composed of seven subunits; Arp2 (actin related protein-2), Arp3, and five additional subunits ArpC1-ArpC5 (Arp2/3 complex component 1-5). Arp2/3 complex binds to existing F-actin filaments by its ArpC subunits and serves as a dock for new G-actin binding onto its Arp2 and Arp3 proteins (Rouiller et al., 2008) (Fig. 3-6). Thus the complex is bound at the pointed end of the newly forming filament and roots a branching at 70°. Activity of the Arp2/3 complex for nucleating a new branch is enhanced by 1) its binding to existing F-actin, 2) phosphorylation at Arp2, and 3) induction with an NPF (nucleation promoting factor). NPFs bind to both Arp2/3 and actin proteins (Fig. 3-6). While class-I NPFs recruit Arp2/3 to the proximity of cellular

membranes and activate them for actin nucleation, class-II NPFs serve for stabilizing the actin filament at the branching points. There are 5 groups of class-I and 2 members of class-II NPFs. Examples of class-I and class-II NPFs are Wasp (Wiscott-Aldrich syndrome protein) and cortactin respectively. In addition to posttranslational regulations, Class-I NPFs are generally inhibited by intramolecular or intermolecular interactions which are relieved by the upstream activators (Lebensohn and Kirschner, 2009); in case of Wasp, Cdc42 relieves the intramolecular autoinhibitory interaction and recruits the Wasp to cell membrane where it activates Arp2/3 for actin nucleation (Tomasevic et al., 2007; Chesarone et al., 2010; Campellone and Welch., 2010).

Formins produce straight F-actin by binding and nucleating at the barbed end of F-actin. Formin proteins are characterized by the presence of FH (formin homology) domains FH1 and FH2. FH2 forms a dimer at the tip of the F-actin and this dimer is sufficient to catalyze actin nucleation (Fig. 3-6). FH1 has proline rich region which serves for recruitment of actin proteins. There are seven subclasses of formins; formins (FMN), Diaphanous-related (Dia), delphilin, formin related proteins in leukocytes (FRL), Dishevelled-associated activator of morphogenesis (DAAM), formin homology domain protein (FHOD) and inverted formins (INF). Among these subclasses, Dia, DAAM, FRL and FHOD has autoinhibitory intramolecular interactions between their DAD (diaphanous autoregulatory domain) and DID (DAD interacting domain) which are at the C-terminus and N-terminus of these molecules respectively. This autoinhibotry interaction is relieved by small GTPase binding to GBD (GTPase binding domain), which generally partially overlaps with the DID region. Small-GTPase binding disturbs the DID-DAD

binding and the FH2 ring becomes available for actin nucleation. Regulation of FMN and INF are not well characterized yet (Chesarone et al., 2010; Campellone and Welch., 2010).

WH2-domain containing nucleators have tandem repeats of G-actin binding domains including WH2 (Wasp homology 2). This group includes Spire, cordon-bleu (COBL) and leiomodin families in mammals. These proteins stabilize the G-actin with their WH2 domains either at the pointed or barbed end of F-actin (Fig. 3-6). Spire1/2 promote actin polymerization in collaboration with FMN by the direct interaction between KIND (kinase non-catalytic C-lobe domain) of spire and FSI (formin-spire interaction) domain of FMN. Similar to spire, Cobl and leiomodin are likely to be interacting with other actin nucleators (Chesarone et al., 2010; Campellone and Welch., 2010; Kerkhoff, 2011).

3.3.2 F-actin regulatory mechanisms during cell division

During cytokinesis of equal cell division, localization of actin bundle and its formation is regulated by Plk1 activity. Small-GTPases have GTP-bound and GDP-bound states which correspond to their active and inactive states. RhoA is an upstream regulator of actin nucleation, and it is activated by Ect2 which is a RhoGEF (guanidine exchange factor), and deactivated by MacRacGAP which is a RhoGAP (GTPase activating protein). Both Ect2 and MacRacGAP are localized at the central spindle and their activities are important during cytokinesis (Tatsumoto et al., 1999; Miller and Bement, 2009). At the equatorial plate, Plk1 is required for the activation Ect2, and by this means contributes to cleavage furrow formation during cytokinesis. GTP-bound RhoA drives cleavage furrow formation and closure by activating Dia and ROCK (Rho kinase). Dia nucleates straight F-actin, and ROCK phosphorylates MLCK (myosin light chain kinase) and activates myosin-II. Thus, the cleavage furrow closure is mediated by the activation of the contractile ring of the actomyosin complex (Glotzer, 2005).

As mentioned above, downstream to RhoA, F-actin formation during cytokinesis of somatic cell division is mediated by the Dia proteins. There are three Dia proteins in mammals: Dia1, Dia2 and Dia3 (Campellone and Welch., 2010). Dia are required for proper spindle formation, actin tubulin organization, cytokinesis and microtubule-kinetochore attachment (Ishizaki et al., 2001; Watanabe et al., 2008; Bartolini et al., 2008; Cheng et al., 2011; Mao, 2011). Dia proteins form homodimers in which their same domains face each other, so that the two FH2 domains form a ring structure (Fig. 3-7). This FH2 ring is located at the barbed-end of the F-actin. Currently it is thought that, FH2 ring

catalyzes F-actin elongation as the FH1 domains recruit the globular actin. As mentioned earlier, Dia proteins have intramolecular DID-DAD interaction which keeps the Dia in its inactive state (Fig. 3-7). This interaction probably prevents, by steric hindrance, the availability of the FH2 ring to F-actin. Binding of small GTPase, RhoA, to the GBD of Dia can relieve the DID-DAD interaction *in vitro*, and this relief maintains activation of Dia by making the FH2 available for binding to the barbed end of F-actin. But since *in vivo* concentration of RhoA is not as high that of in vitro experiments (Lii and Higgs., 2003), it is anticipated that RhoA is not sufficient and there must be some other regulators for Dia activation. Nonetheless, RhoA binding enhances activation of Dia and more importantly determines the localization of Dia at the cleavage furrow during cytokinesis (Campellone and Welch, 2010).

3.3.2.1 F-Actin regulation during PBE

In animals that have their GV at the center of immature oocytes, as mentioned earlier, spindle must be moved from the center to the cortex of the oocyte (McCarthy and Goldstein, 2006; Azoury et al., 2011). This is maintained by the involvement of the branched F-actin nucleator, the Arp2/3 complex, and the straight F-actin nucleators, Formin-2 and Spire1/2 proteins (Chaigne et al., 2013; Dumont et al., 2007; Campellone and Welch, 2010; Pfender et al., 2011). Although not much is known about the upstream regulators of Formin-2 and Spire1/2, the activation of Arp2/3 is mediated by the small-GTPases, Cdc42 and Rac1. Small GTPases binds to the class-I NPFs of the Arp2/3 complex, which are kept in their inactive states through intramolecular (as in WASP) or intermolecular interactions (as in WAVE). Binding of small-GTPases activates the NPFs via relieving their inhibitory interactions and also regulates their localizations (Campellone and Welch, 2010). Together with these actin nucleators, non-muscle myosin-II is also involved in the spindle movement to the oocyte cortex (Simerly et al., 1998; Schuh and Ellenberg, 2008; Yi and Li, 2012).

In animals that have their GV at the animal pole in immature oocytes, the spindle is formed under the oocyte cortex. However the long axis of the spindle is not always perpendicular to the oocyte cortex. To maintain perpendicular orientation, one spindle pole is attached to the cortex, in an unknown mechanism, and the spindle is rotated through RhoA mediated F-actin formation (Gard, 1992; Zhang et al., 2008). Myosin-II contractility and Aurora A activity is also required in spindle rotation (Castro et al., 2003).

During metaphase, eccentric localization of the spindle drives polarization of the oocyte cortex that leads the formation of a cortical differentiation which is resultantly represented by the presence of F-actin cap (Cowan, 2007; Halet and Carroll, 2007). A RanGTP gradient is shown to be the main factor that regulates the cortical organization in metaphase-II arrested oocytes (Deng et al., 2007), but involvement of RanGTP during metaphase-I is also anticipated for cortical organization. Close proximity of spindles to the animal pole causes the distinct localization patterns of several proteins at the animal pole cortex; the small-GTPases, Rac1 and Cdc42 localizes at the spindle attachment point while RhoA, another small-GTPase forms a ring around them (Fig. 3-5) (Benink and Bement, 2005; Halet and Carol, 2007; Liu, 2012). Cdc42 is an activator of Wasp, thus it is an upstream regulator of Arp2/3, and localization of Cdc42 mediates branched F-actin formation at the spindle attachment point which causes a protrusion at and around the spindle attachment point during anaphase. Rac1 and Cdc42 are also included, probably by regulating Arp2/3 activity, in proper meiotic spindle formation, and in spindle migration and attachment to the cortex together with a RanGTP gradient (Benink and Bement, 2005; Zhang et al., 2008). On the other hand, RhoA is an upstream regulator of straight F-actin nucleation, and its localization around the Cdc42 region at the cortex mediates F-actin ring during cleavage furrow formation around the protruded region which then might be driving the cleavage furrow closure (Fig. 3-5) (Bement et al., 2005; Ma et al., 2006). Consistently, a myosin-II ring is established around the protrusion which drives the constriction of the actomyosin ring (Zhang et al., 2008; Deng and Li, 2009; Maddox et al., 2012). F-actin nucleators Formin-2 and Spire1/2 proteins,

that are not regulated by RhoA, was shown to be localized and driving the F-actin formation at the cleavage furrow (Dumont et al., 2007; Campellone and Welch, 2010; Pfender et al., 2011), but the downstream effectors of RhoA are not yet shown to be involved in actin ring formation. Although the budding yeast Diaphanous-related formins, Bni1 and Bnr1, are important for unequal cell division (Sagot et al., 2002; Gao et al., 2010), regulation and roles of Dia proteins in PBE have not been studied.

3.4 The Mos-MAPK-p90Rsk pathway in oocyte maturation

c-Mos is a serine/threonine kinase which functions in meiotic division. Although immature oocyte contains Mos mRNA, its expression is induced by a polyadenylation dependent mechanism upon activation of CycB-Cdk1. Accumulation of Mos protein activates the MAPK via MEK around the time of GVBD in most animals (starfish, cnidarians and mammals), and then MAPK activates p90Rsk. After its activation, Mos-MAPK-p90Rsk pathway remains activated throughout the oocyte maturation and inactivated after fertilization.

The most fundamental role of the Mos-MAPK-p90Rsk pathway is to maintain the second meiotic arrest (Fig. 3-8). After fertilization the Mos is degraded and the MAPK-p90Rsk pathway is inhibited (Sagata et al., 1989; Haccard et al., 1993; Kosako et al., 1994; Bhatt and Ferrel, 1999; Gross et al., 1999). As mentioned before, second meiotic arrest might occur at different stages during oocyte maturation and these different stages give us hints about the detailed functions of the Mos-MAPK pathway. In vertebrates, the second meiotic arrest is at metphase-II and Mos-MAPK pathway is required for maintaining the CycB-Cdk1 activity high during this arrest until fertilization takes place. Erp1/Emi2 (Emi1 related protein-1/ Early mitosis inhibitor-2) protein accumulates after meiosis-I, binds and inhibits APC/C to prevent CycB degradation. p90Rsk phosphorylates Erp1/Emi1, and mediates its stabilization and its binding to APC/C (Inoue et al., 2007; Nishiyama et al., 2007). In echinoderms the second meiotic arrest is at G1 phase of the first mitotic division (Tachibana et al., 1997; Kumano et al., 2001; Mori et al., 2006). These oocytes are prevented from replicating their DNA before fertilization (Tachibana et al., 1997). In G1-arrested oocytes DNA replication machinery is

stopped at pre-RC (pre-replication complex) stage in which the MCM (minichromosome maintenance, the helicase) is loaded on DNA but not activated (Bell and Dutta, 2002). Although the direct substrate for p90Rsk is yet to be found, it is shown that activity of the Mos-MAPK-p90Rsk pathway prevents loading of Cdc45 onto DNA, which is the critical factor for triggering the helicase activity (Tachibana et al., 2010). In addition, MAPK but not the p90Rsk is responsible for the prevention of M-phase entry at G1-arrest (Hara et al., 2009).

Another essential function of the Mos-MAPK pathway is to maintain meiosis-I to meiosis-II transition (Fig. 3-8). Basically Mos-MAPK pathway favors the fast CycB synthesis after completion of meiosis-I for the CycB-Cdk1 reactivation. In *Xenopus* and starfish, although the oocyte gains all the equipment for DNA replication during maturation, the Mos-MAPK pathway prevents DNA replication after meiosis-I and forces the oocyte for entry into meiosis-II. Prevention of Mos or inactivation of MAPK in the oocytes of these animals cause S-phase entry and the oocytes enter parthenogenesis after meiosis-I (Gross et al., 2000; Tachibana et al., 2000; Dupré et al., 2002; Dupré et al., 2011).

The Mos-MAPK pathway might be involved in earlier stages during meiotic maturation because inhibition of MAPK activity in immature oocytes by treatment with a MEK-specific inhibitor (U0126) alters the activities of cell cycle regulators during oocyte maturation (Fig. 3-8) (Okano-Uchida et al., 2003). Yet, the role of the Mos-MAPK-p90Rsk pathway during PBE has not been studied in detail in starfish oocytes. In other organisms, conflicting results were obtained whether the Mos-MAPK pathway functions in PBE. Inhibition of Mos1

but not Mos2 ortholog in cnidarian oocytes by morpholino oligonucleotide injection at GV stage prevents PBE (Amiel et al., 2009). On the other hand, Mos knock-out (Mos-KO) mouse oocytes extrude abnormally big polar bodies and enter parthenogenesis (Choi et al., 1996; Verlhac, 2000), but injection of Mos antisense oligonucleotides (MosAS) (Paules et al., 1989) at GV stage prevents PBE in wild type mouse oocytes. In contrary to these conflicts, inhibition of MEK activity by U0126 at GV stage prevents PBE consistently in cnidarian, mouse and pig oocytes (Lee et al., 2000; Lee et al., 2007; Amiel et al., 2009). However, ambiguous results were obtained by MEK inhibition following GVBD in mouse oocytes: emission of normal polar bodies, large polar bodies, polar bodies without chromosomes or no polar bodies (Tong et al., 2003; Lee et al., 2007). In summary, there are some contradictions about the role of Mos-MAPK in polar body emission in different organisms, and the role of Mos-MAPK during PBE is not observed in starfish oocytes yet.

3.5 The purpose of this study

During oocyte maturation, although the roles of some cell cycle regulators are known, their downstream targets are generally unknown. Although, the Mos-MAPK-p90Rsk pathway, a meiosis specific cell cycle regulatory pathway, has been studied in detail during secondary oocyte arrest, its roles during earlier steps of oocyte maturation are not well described yet. In this study, in addition to the elucidation of the role of the Mos-MAPK pathway in PBE, I have also aimed to elucidate a downstream target of this pathway.

To clarify the requirement of the Mos-MAPK-p90Rsk pathway in PBE in starfish oocytes, I have used live-cell imaging. Use of live-cell imaging enhances our understanding to monitor the fate of single oocytes, thus the roles of the Mos-MAPK-p90Rsk pathway during PBE could be reliably described. Based on the described roles of the Mos-MAPK-p90Rsk pathway, at the next step, I have concentrated to clarify a downstream target of the pathway. I have concentrated on the regulation of actin nucleation and polymerization. Among actin nucleators, due to its roles in cytokinesis in somatic cells and budding of the yeast, I have aimed to investigate whether localization and activation of starfish Dia is regulated by the Mos-MAPK pathway during cleavage furrow closure. This investigation, for the first time, establishes the connection between the Mos-MAPK pathway and the regulation of contractile ring formation during PBE.

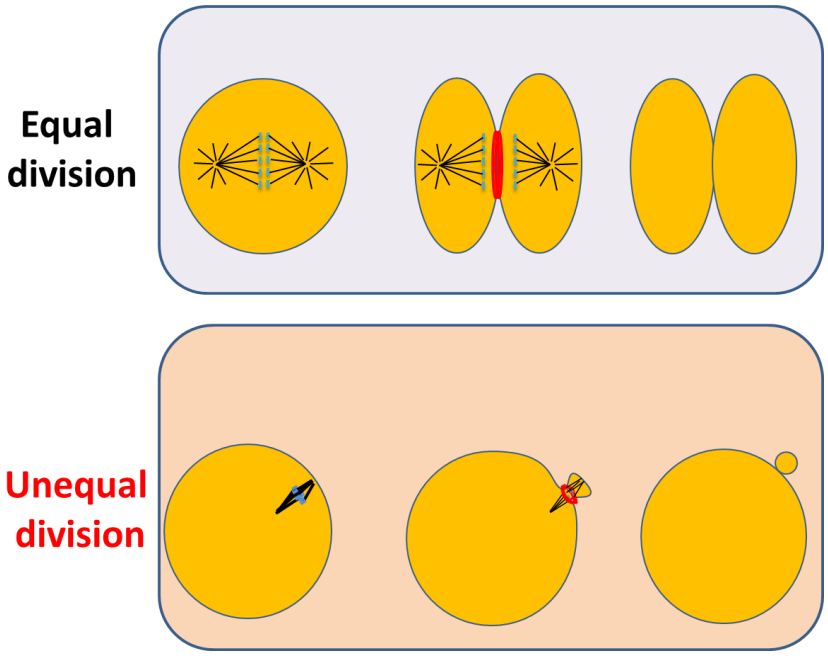

Fig. 3-1. Equal cell division vs unequal cell division. Different from equal cell division, in unequal cell division that results in differently sized daughter cells, the spindle is positioned eccentrically, and then the cleavage furrow positioning correlates with the position of the spindle.

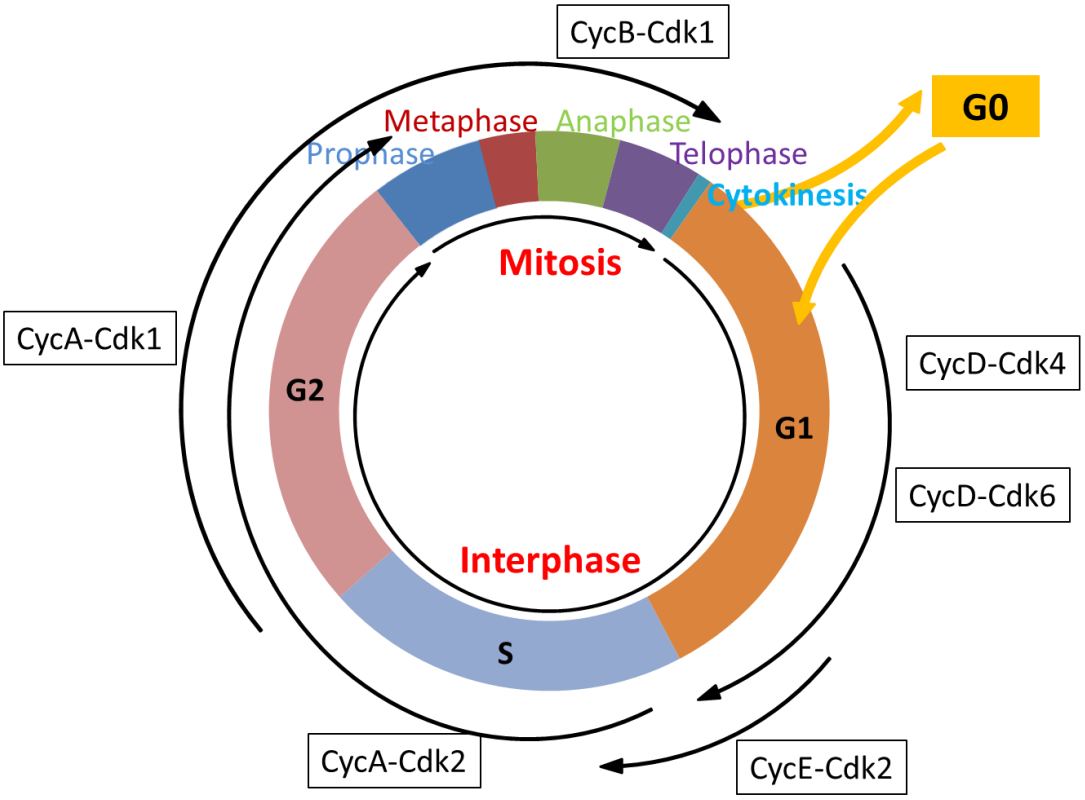

Fig. 3-2. Mitotic cell division cycle.

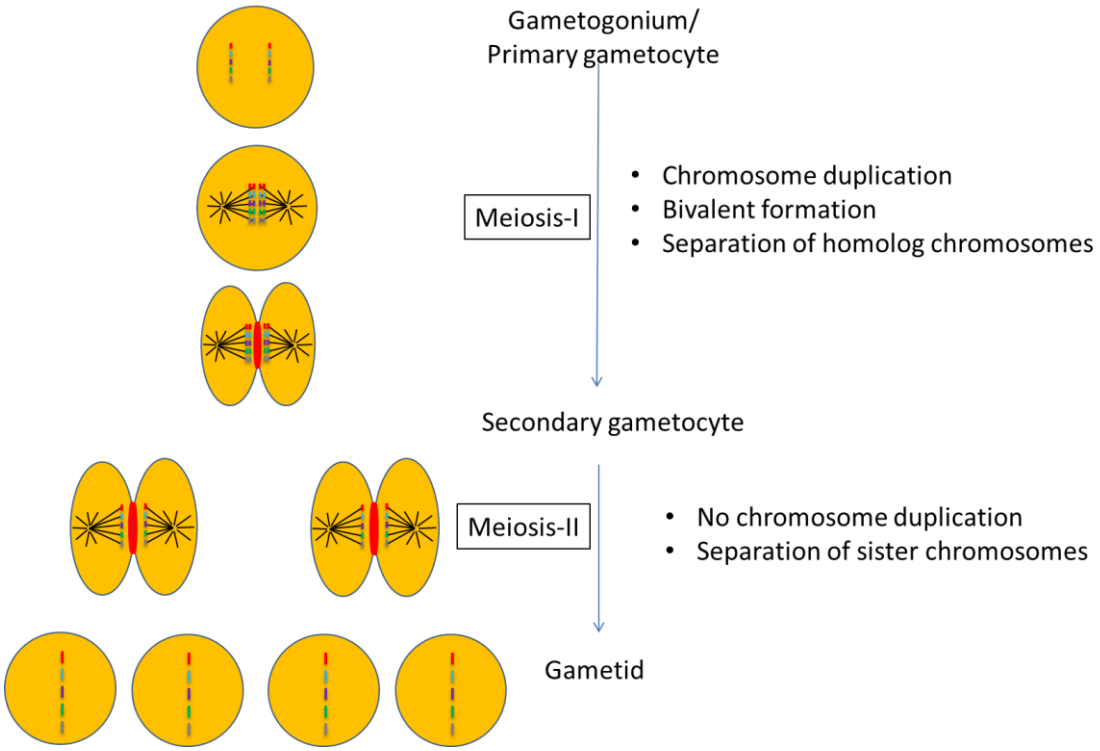

Fig. 3-3. Meiotic cell division

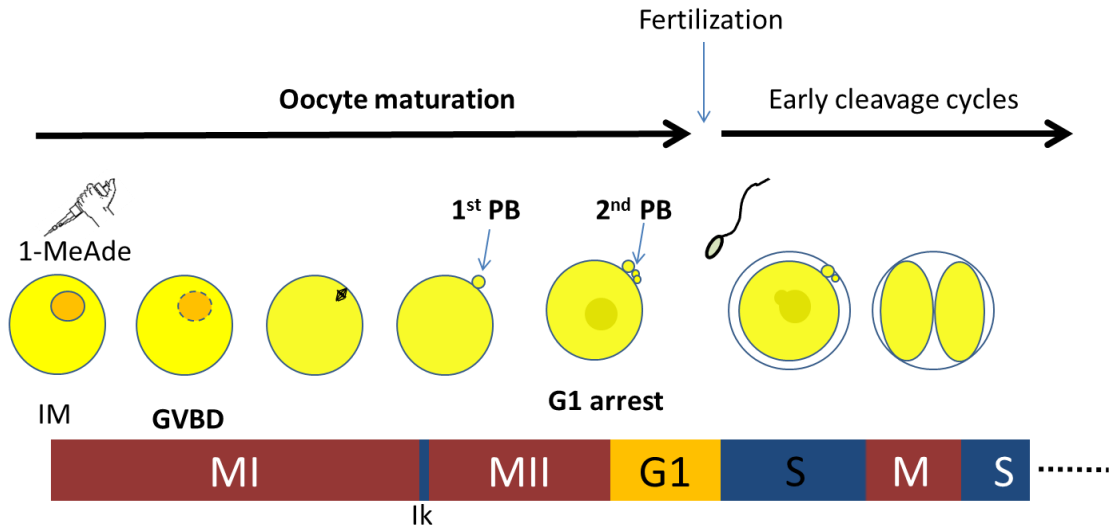

Fig. 3-4. Oocyte maturation of starfish. Immature oocytes are arrested at prophase of meiosis-I. Upon treatment with 1-methyladenin, maturation inducing hormone, oocyte maturation starts, germinal vesicle breaks down (GVBD), spindle forms under the cortex, first and second polar bodies (PB) are extruded, and then oocytes are arrested at G1 phase awaiting fertilization. Upon fertilization early developmental cleavage cycles start.

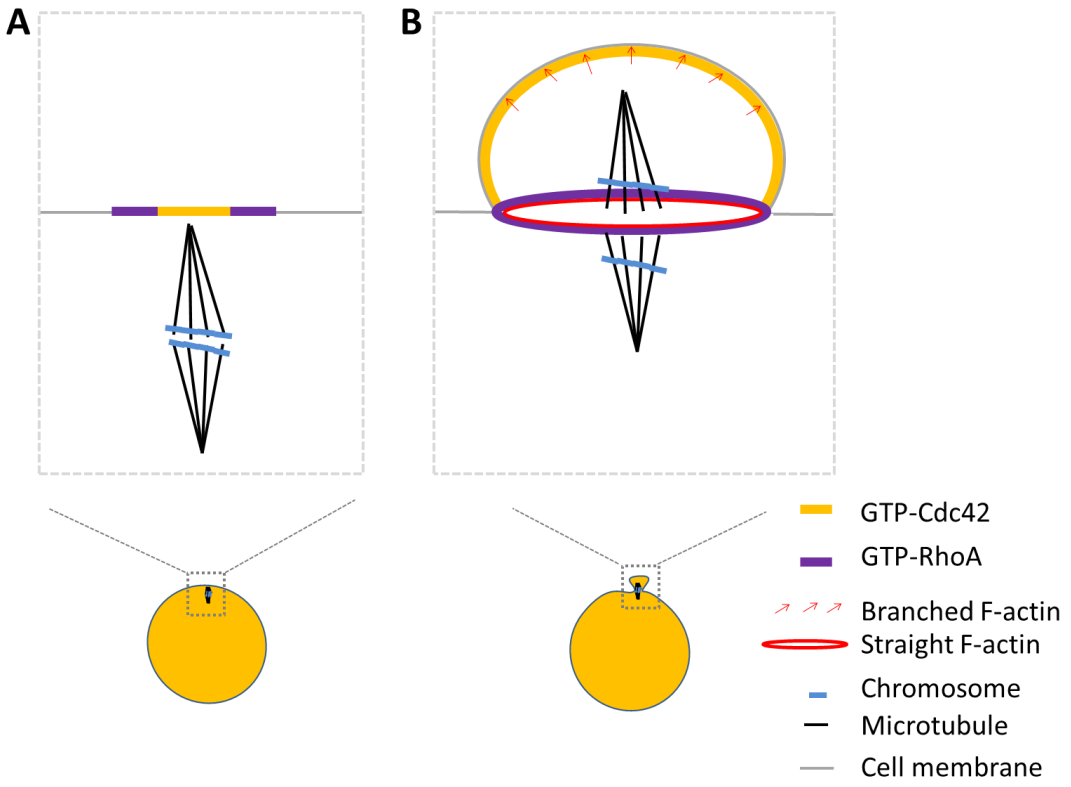

Fig. 3-5. Polar body emission. A) In oocytes, at the end of M-phase, spindle is positioned under the cortex perpendicularly to the oocyte cortex. Active Cdc42 is localized at the spindle attachment region, active RhoA encircles active Cdc42. B) In anaphase, branched F-actin formation via Cdc42 mediated Arp2/3 complex activation leads to a membrane protrusion into which one spindle pole and half of the genetic material is emitted. Then, straight F-actin formation via RhoA dependent mechanism drives the contractile ring and the cleavage furrow formations in between separated chromosomes.

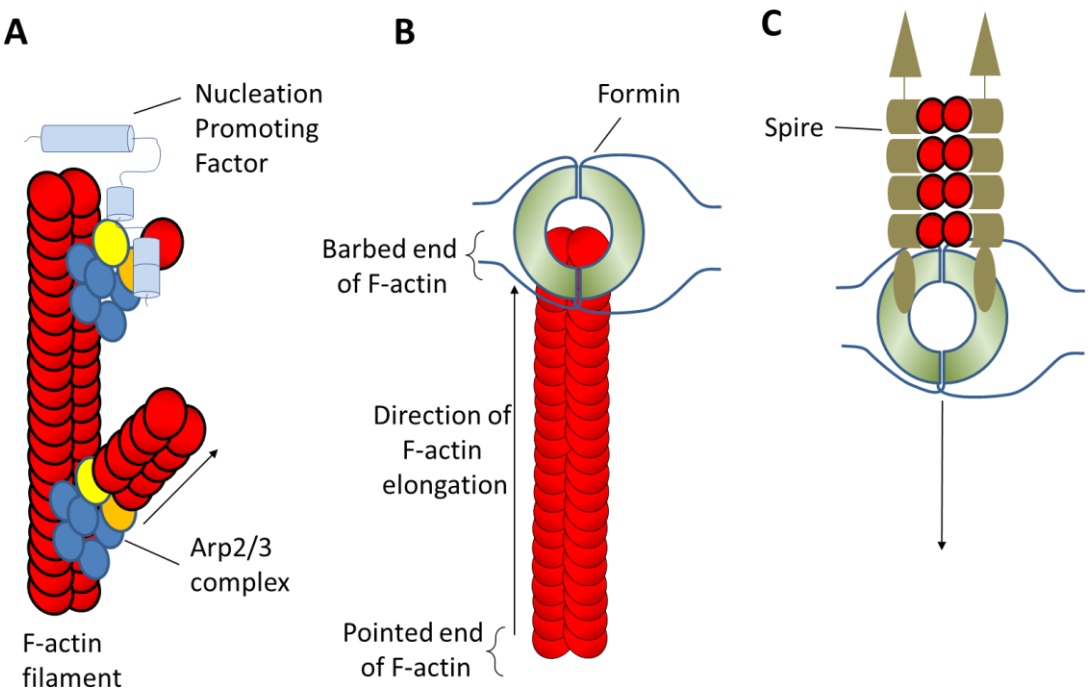

Fig. 3-6. F-actin nucleation mechanism. A) Arp2/3 complex binds on preexisting F-actin filaments and, by the aid of NPFs, roots branching of the F-actin filaments at the pointed ends. B) Formin family proteins nucleate straight actin filaments by adding actin monomers at the barbed end of the F-actin. C) Spire family proteins cooperate with formins and root straight F-actin nucleation at the pointed end of F-actin.

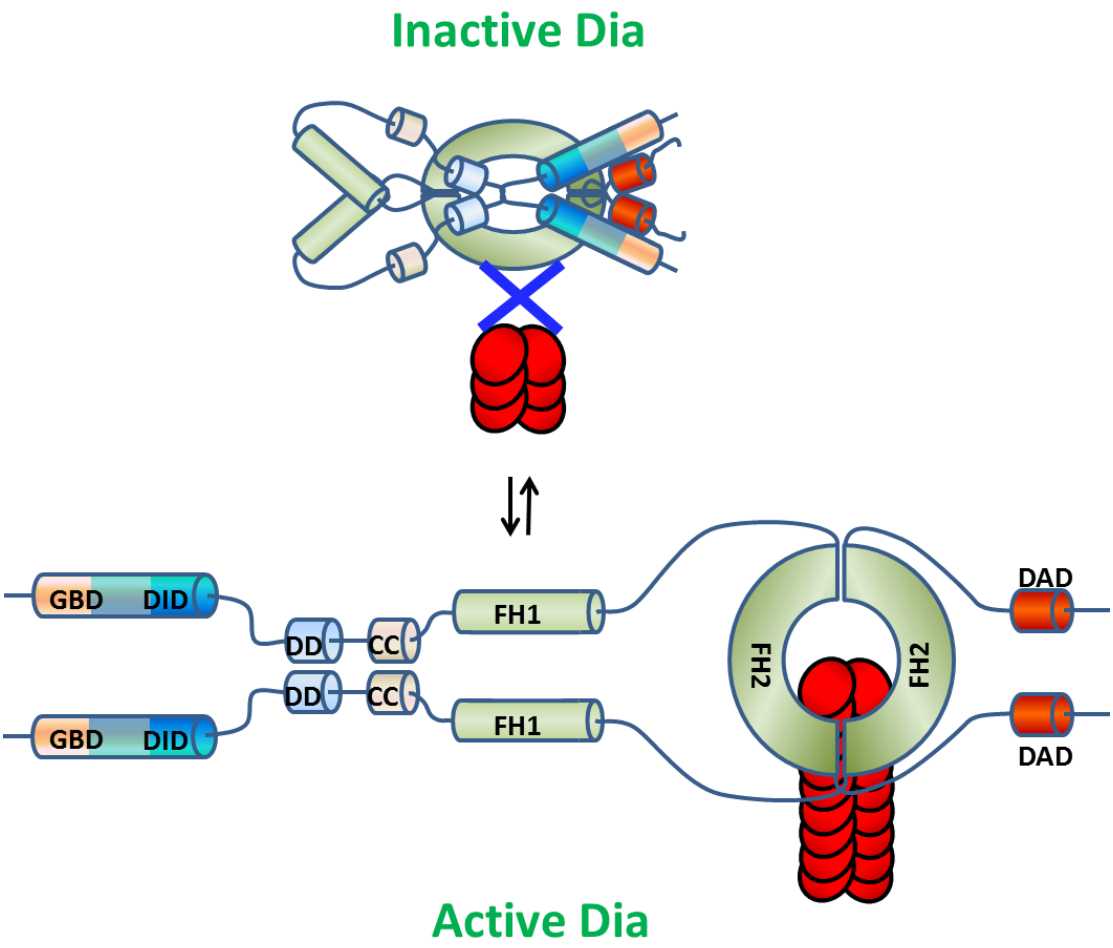

Fig. 3-7. Domain structure of Diaphanous related formin (Dia). Dia forms functional homodimers and functions for contractile ring formation during cytokinesis. The FH2 ring cannot function in the inactive form in which the DAD and DID are interacting with each other. Upon activation via RhoA binding to GBD and additional factors, DAD-DID interaction is relieved and the FH2 ring becomes available for actin nucleation.GBD, GTPase binding domain; DID, DAD interacting domain; DD, dimerization domain; CC, coiled coil; FH1, formin homology 1; FH2, formin homology 2; DAD, Dia autoregulatory domain.

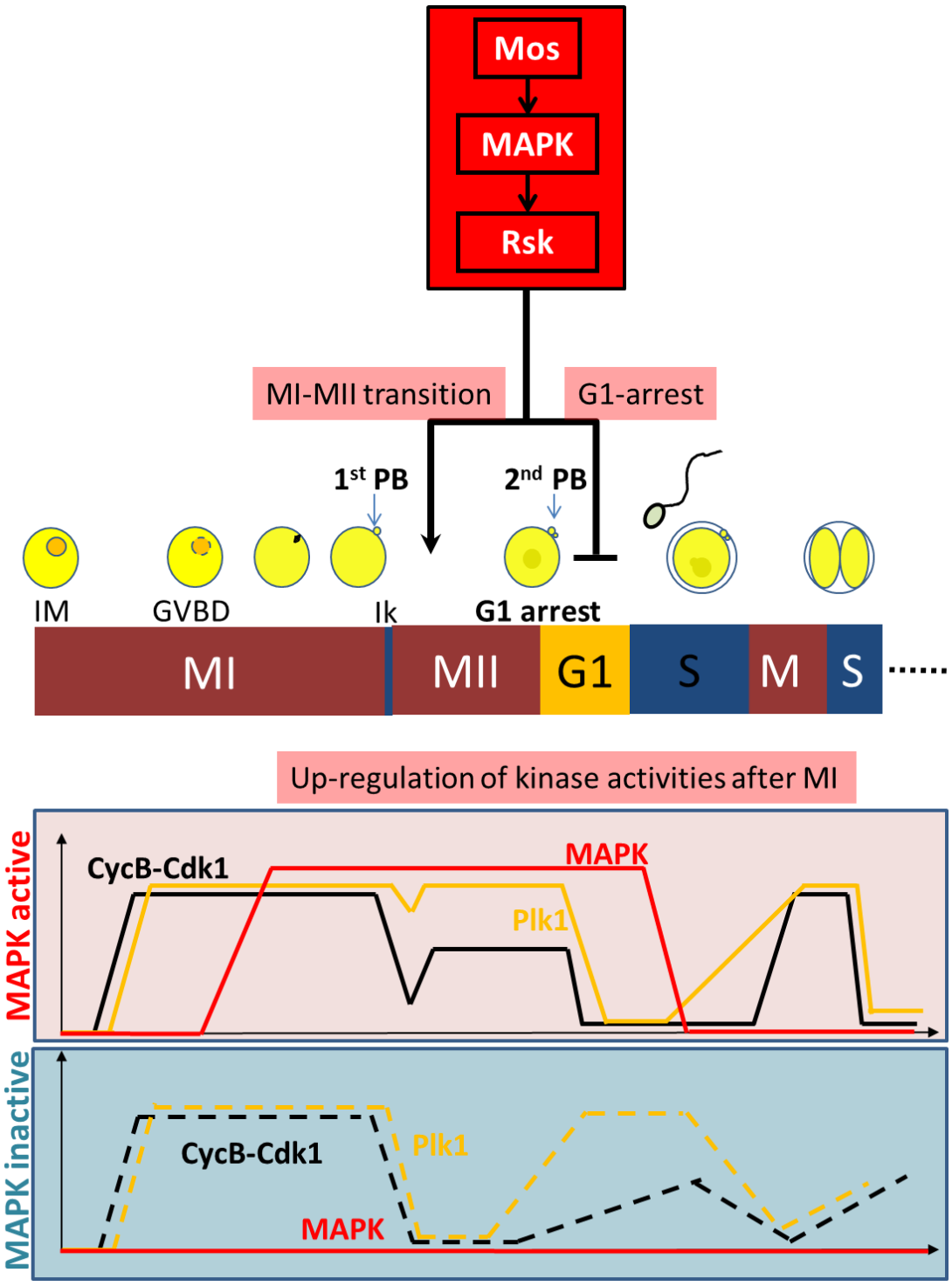

Fig. 3-8. Roles of the Mos-MAPK pathway during oocyte maturation in starfish. The Mos-MAPK pathway is activated at around GVBD, remains active during oocyte maturation, and maintains MI-MII transition and G1 arrest. Mos-MAPK activity is also required for proper kinase activities after completion of meiosis-I.

4. RESULTS

4.1 Mos-MAPK-p90Rsk pathway regulates PBE

4.1.1 Section Summary

In this section the requirement of the Mos-MAPK-p90Rsk pathway for PBE in starfish oocytes was examined, and the roles of this pathway was characterized. To do so, here, I have injected the oocytes with HiLyte-488-labeled tubulin and Alexa-568-labeled histone-H1, and then observed spindle dynamics and PBE during oocyte maturation in the presence or absence of Mos, MAPK or p90Rsk activities.

To inhibit Mos synthesis, antisense oligonucleotide against Mos was injected into immature oocytes. For inhibition of MAPK activity, a MEK-specific chemical inhibitor, U0126, was used to examine the requirement of MAPK activity for PBE. And a constitutively active p90Rsk protein was injected into immature oocytes to examine whether p90Rsk can recover from the defects in the absence of MAPK activity.

In the experiments of both Mos- and MAPK-inhibitions, I have found that Mos or MAPK activities are not required for the spindle formation or migration to the oocyte cortex; but during PBE, maintenance of tight spindle attachment to cortex, proper chromosome separation and cleavage furrow closure require Mos and MAPK activities. Finally, it was clearly shown that all defects caused by MAPK inhibition were recovered by p90Rsk.

4.1.2 Mos is required for PBE

To examine the role of Mos in PBE in starfish oocytes, fully-grown (see below) immature oocytes were injected with control oligonucleotide or MosAS, which prevents Mos synthesis in starfish (Tachibana et al., 2000), and then meiotic maturation was induced by treatment with 1-methyladenine (1-MeAde, starfish maturation-inducing hormone). All oocytes injected with MosAS failed in PBE whereas control oocytes emitted PBs (Fig. 4-1A).

Live-cell imaging was used to examine the effect of Mos on spindle and chromosome dynamics. Fully-grown immature oocytes were microinjected with HiLyte-488-labeled tubulin (green) and Alexa-568-labeled histone-H1 (red) (Hara et al., 2012), together with control oligonucleotide or MosAS and then meiotic maturation was induced.

In control oocytes, the spindle was formed in GV region under the cortex, moved slightly towards cortex (data not shown). And then, the spindle attached to the cortex and rotated, meanwhile chromosomes were aligned at the metaphase plate (Fig. 4-1B, 56–66 min). Upon completion of spindle orientation, the spindle was pushed against the animal pole (spindle repositioning), which caused the animal pole to move outwards, meanwhile chromosome separation began, indicative of anaphase (Fig. 4-1B, 73 min). After completion of chromosome separation, the animal pole was pulled back, but the spindle was kept relatively distant, resulting in formation of a protrusion (Fig. 4-1B, 81 min, arrow).Upon completion of chromosome separation, the cleavage furrow began to close in the region between the chromosomes, and then abscission of the cleavage furrow was completed, resulting in the first PBE (Fig. 4-1B, 81–85 min). Thereafter, the second meiotic spindle formed in

the same region and the second polar body was emitted (Fig. 4-1B, 91 min).

On the other hand, when the oocytes were injected with MosAS, although spindle oriented under the cortex and spindle repositioning started similarly with control oocytes (Fig. 4-1C, 49–69 min), there were several defects; 1) the protrusion was larger than that of control oocytes (Fig. 4-1C, 72–78 min), 2) the spindle pole was not closely attached to the cortex (Fig. 4-1C, 75–78 min, two sided arrows) and 3) chromosome separation was not properly organized (Fig. 4-1C, 69–78 min). Despite these defects, chromosomes separated completely (Fig. 4-1C, 75–96 min), but the cleavage furrow did not close (Fig. 4-1C, 103–122 min). As a result, PBE failed, the separated chromosomes gathered together and multipolar spindles formed, after which parthenogenesis began as described previously (Tachibana et al., 2000).

4.1.3 MAPK activity is required for PBE

To examine the effects of MAPK activity on PBE, MEK-specific inhibitor, U0126, was used. First, to determine the effective concentration of U0126 on MAPK activation, oocytes were collected at 60 min after addition of 1-MeAde to immature oocytes in the presence of different concentrations of U0126, and western blotting was performed for MAPK and p90RSK, a kinase downstream of MAPK (Mori et al., 2006). MAPK and p90Rsk migrated at higher molecular weights (activated forms) at 60 min in DMSO treated oocytes, however, this was prevented by treatment with 2.5 μM and higher concentrations of U0126 (Fig. 4-2A). Next, oocytes were collected at 10 min intervals after treatment with 1-MeAde in the absence or presence of 3.5 μM U0126. Consistent with previous results (Okano-Uchida et al., 2003), MAPK and p90RSK were activated at 30 min after 1-MeAde treatment, however, this was prevented by treatment with 3.5 μM U0126 (Fig. 4-2B). Finally, oocytes that were induced for meiotic maturation in the presence of different concentrations of U0126 were examined for PBE. It was observed that 3.5 μM U0126, but not 1 μM U0126, prevents PBE in 100% of oocytes (Fig. 4-2C). On the other hand, higher levels of U0126 (10 μM) was required to prevent PBE when treatment was done after GVBD (data not shown). This phenomenon suggests that the differences in the reports of Tong et al., 2003; Lee et al., 2000; Lee et al., 2007; Yu et al., 2007 might be dependent on the timing and concentration of U0126 treatment. Size of the protrusion was measured in U0126-treated and control oocytes, and it was observed that U0126-treatment causes ~2.5 times increase in protrusion size (Fig. 4D).

To observe the effect of MAPK inhibition on spindle dynamics and PBE,

live-cell imaging was performed. DMSO-treated control oocytes succeeded in PBE (Fig. 4-3A). In contrast, when oocytes were treated with 3.5 μM U0126, there were defects during the spindle repositioning and these defects were similar with MosAS injected oocytes; large protrusion (Fig. 4-3B), non-tight spindle pole attachment to the cortex, and non-proper chromosome separation (Fig. 4-3B, 47–54 min). Despite these defects, similar to MosAS injected oocytes, chromosomes once separated completely (Fig. 4-3B, 58 and 62 min), but the cleavage furrow did not close (Fig. 4-3B, 51–62 min), and the separated chromosomes gathered together, and then multipolar spindles formed (Fig. 4-3B, 68–92 min)

4.1.4 p90Rsk performs functions of MAPK during PBE

Both to examine the involvement of p90Rsk in PBE and to exclude the possibility that U0126 may have side effects, oocytes were injected with constitutively active p90Rsk (CA-Rsk) or kinase dead p90Rsk (KD-p90Rsk) (Hara et al., 2009), treated with 20 μM U0126 (8 times higher than the minimum effective concentration of U0126), and then induced for maturation. It was observed that all oocytes that were injected with CA-p90Rsk rescued PBE but KD-p90Rsk injected oocytes did not (Fig. 4-4A). When oocytes were examined by live-cell imaging it was observed that, in the presence of 20 μM U0126, CA-p90Rsk was able to recover all the defects caused by U0126-treatment and rescue PBE (Fig. 4-4B) whereas KD-p90Rsk injected oocytes had similar phenotypes with non-injected oocytes (Fig. 4-4C). These data indicate that U0126-treatment is specific to Mos-MAPK pathway at least until 20μM and exclude the possibility of side effect involvement in the observed defects in 3.5 μM U0126-treated oocytes. The rescue of PBE by CA-p90Rsk seems conflicting with a previous data (Mori et al., 2006) which reports PBE in neutralizing anti-p90Rsk injected oocytes, but I suspect that since the neutralization of p90Rsk activity was not 100%, a well localized high p90Rsk activity could account for PBE.

4.2 Dia activity downstream of MAPK is required for PBE

4.2.1 Section summary

In this section, to clarify a downstream target of the Mos-MAPK pathway during cleavage furrow closure, I have concentrated on the actin regulatory mechanisms. First, I have investigated that the FH2 domain activity is required for cleavage furrow closure during PBE; second, I have cloned starfish Dia (ApDia), and then determined the localization of ApDia at the cleavage furrow during PBE; third, I have activated endogenous ApDia in the absence of the MAPK activity to observe whether ApDia activity is sufficient for cleavage furrow closure; lastly, I have constructed a novel constitutively active ApDia mutant, and expressed this mutant in the oocytes to observe whether it can drive cleavage furrow closure in the absence of MAPK activity.

To inhibit FH2 activity a small molecule inhibitor of FH2 (SMIFH2) was used. To observe localization of ApDia, GFP2-ApDia mRNA was expressed in the immature oocytes and GFP2 signal was monitored during oocyte maturation and PBE in the presence or absence of MAPK activity. To activate endogenous ApDia, GST-tagged DAD or GBD/DID of ApDia or GFP-tagged GBD/DID of mDia1 peptides were injected into immature oocytes. To construct a novel constitutively active ApDia, the DAD was mutated into a non-related amino acid sequence by inserting two frame-shift mutations at the beginning and at the end of DAD resulting in constitutively active ApDia with a frame-shifted DAD (GFP2-ApDia-fsDAD).

To sum up, I have found that the fine localization of ApDia at the cleavage furrow is regulated by the Mos-MAPK pathway. Both the experiments of activation of endogenous ApDia and expression of constitutively active

ApDia mutants show that in the absence of MAPK activity, Dia activity is sufficient to drive cleavage furrow closure. Thus, it was demonstrated that the Mos-MAPK pathway regulates both the localization and activation of the ApDia during PBE in starfish oocytes. To note, this is the first elucidation on a connection between Dia and the Mos-MAPK pathway.

4.2.2 FH2 activity is required for PBE

Although chromosomes separated in Mos- or MAPK-inhibited oocytes, the cleavage furrow failed to close. I further examined this main defect, which might be related to contractile ring formation and thus straight actin nucleators (Barr and Gruneberg, 2007; Fededa and Gerlich, 2012). To determine whether formin proteins are involved in cleavage furrow closure during PBE, oocytes were treated with 100 μM SMIFH2, a specific inhibitor of the formin homology (FH) 2 domain (Rizvi et al., 2009). To avoid perturbation of GVBD and to ensure correct spindle formation, SMIFH2 treatment was performed after GVBD (30 min after the treatment with 1-MeAde). In these oocytes, the spindle aligned properly under the cortex and chromosomes separated normally (Fig. 4-5, 52–72 min); however, the cleavage furrow did not close completely and separated chromosomes gathered together (Fig. 4-5, 83–100 min). The phenotypes of SMIFH2-treated and Mos- or MAPK-inhibited oocytes were very similar regarding cleavage furrow closure, although the phenotype of SMIFH2-treated oocytes was relatively milder.

4.2.3 Cloning of ApDia

The above mentioned similarity in the phenotypes indicates there is a connection between the Mos-MAPK pathway and formins. SMIFH2 inhibits all FH2 domain-containing proteins. However, I chose to concentrate on Dia proteins because the cleavage furrow did not close completely in perturbed oocytes and mDia1 and mDia2 are located at the cleavage furrow and are required for completion of cytokinesis in somatic cells (Watanabe et al., 2008; Watanabe et al., 2010). Moreover, Bni1 and Bnr1, Dia counterparts in yeast, are required for completion of budding, a well-studied type of unequal cell division (Evangelista et al., 1997; Yu et al., 2011; Chen et al., 2012).

Only a single Dia gene has been identified in the ongoing starfish genome project organized by this laboratory in collaboration with Prof. Takehiko Itoh, despite higher organisms having three Dia genes. This is a common phenomenon when comparing genes in echinoderms and higher organisms (Abe et al., 2010). ApDia was cloned from a cDNA library of immature *A. pectinifera* oocytes (Fig. 4-6), indicating that ApDia is expressed in immature oocytes.

ApDia amino acid sequence shows 34%, 36% and 37% identity, and 50%, 55% and 55% similarity to, those of mammalian homologs; mDia1, mDia2 and mDia3 respectively. This indicates that ApDia represents all mDia proteins as a single protein. Detailed investigation of ApDia further supports this idea that ApDia shares identity with different mDia proteins at different residues even in the same regions (please see the explanation in Fig. 4-6). The ApDia sequence was uploaded into Pubmed Genebank and the accession number of ApDia is KC701713.

4.2.4 MAPK regulates ApDia localization to cleavage furrow

To identify the localization of ApDia protein in oocytes, HA-GFP2-ApDia mRNA was injected into immature oocytes. Five hours later, GFP2-ApDia fluorescence in the immature oocytes was examined by confocal microscopy. Fluorescence was intense at the cortex, weak in the cytoplasm and absent from the GV region (Fig. 4-7A, upper plane). Interestingly, when a thinner confocal plane was used, GFP2-ApDia was absent from a region in the animal pole cortex (Fig. 4-7A, lower plane). Construction of a 3D view of this region shows a hole-like GFP2-ApDia absent region (Fig. 4-7B). This region is the spindle attachment region at which PBE occurs. This data indicates that cortical organization and distinct distributions of cortical proteins are already established in immature starfish oocytes, unlike mouse oocytes (Azoury et al., 2009). Expression of HA-GFP2-ApDia at the expected molecular weight was confirmed by western blotting with an anti-HA antibody (Fig. 4-7C).

Next, to examine whether ApDia localizes to the cleavage furrow, maturing oocytes expressing HA-GFP2-ApDia was examined by confocal microscopy. After GVBD, GFP2-ApDia fluorescence slightly and transiently increased in the GV area (data not shown). Following spindle formation, attachment and rotation, GFP2-ApDia concentrated around the spindle (data not shown). During anaphase GFP2-ApDia was absent from the cortex of protrusion and concentrated at the cleavage furrow (Fig. 4-8, 52–59 min) indicating that ApDia forms a ring at the cortex around the spindle. Consistent with this notion, GFP2-ApDia concentrated and closed with cleavage furrow (Fig 4-8, 60–65 min). This localization of ApDia is consistent with its role in cleavage furrow formation (Watanabe et al., 2008).

By using a thicker confocal plane, GFP2-ApDia enrichment at the cleavage furrow during PBE was quantified (Fig. 4-9A). It was observed that GFP2-ApDia localization at the presumptive PBE region increased when spindle attached to the cortex and peaked at the time of cleavage furrow formation (Fig. 4-9B, see -17 min and 0 min, respectively). In average, 1.67 times higher GFP2-ApDia signal at the cleavage furrow than that of control cortex was observed (Fig. 4-9C). To our knowledge, this is the first data reporting localization of a Dia protein at the cleavage furrow during meiotic division.

Next, the localization of HA-GFP2-ApDia protein in MAPK-inactivated oocytes was examined. In maturing oocytes that were treated with 3.5 μM U0126, GFP2-ApDia localization was similar to control oocytes until spindle repositioning (data not shown). And then, in contrast to control oocytes, first of all, GFP2-ApDia concentrated at around the protrusion and the GFP2-ApDia absence at the protrusion was lost (compare Fig. 4-8, 59–65 min with Fig. 4-10, 63–95 min). Secondly, although higher GFP2-ApDia signals at certain points (possible cleavage furrow region) were observed (Fig. 4-10, 71–85 min, arrowheads); they were not concentrated, which may be parallel with the failure of the cleavage furrow closure (Fig. 4-10, 106 min). These data show that fine localization pattern of GFP2-ApDia is controlled by MAPK.

4.2.5 PBE rescue by activation of endogenous ApDia

Since furrow closure was not observed, although GFP2-ApDia was present at around the cleavage furrow, I suspected that activation of ApDia in addition to its localization might be controlled by MAPK, and that both localization and activation disturbances might be responsible for PBE failure in U0126-treated oocytes.

To test this idea, first, I aimed to activate endogenous ApDia protein in MAPK-inactivated oocytes. Previous reports showed that exogenous DAD expression competes with the DAD of endogenous Dia, prevents the intramolecular DID-DAD interaction and thereby activates endogenous Dia (Palazzo et al., 2001). Thus, I injected GST-ApDia-DAD protein (amino acids 1004–1105) into immature oocytes, and then induced meiotic maturation in the presence of 3.5 μM U0126. When examined by live-cell imaging, surprisingly, all three defects observed following Mos-MAPK inhibition were rescued in these oocytes; 1) the protrusion was not large, 2) the spindle was closely attached to the cortex, and 3) chromosomes aligned and separated properly (Fig. 4-11, 59–72 min). Finally, the cleavage furrow closed completely, resulting in the first PBE (Fig. 4-11, 75–97 min), after which the oocyte entered parthenogenesis (data not shown).

Currently known formins which have DID-DAD interaction are FHOD (FH1/FH2 domain-containing protein), FRL (Formin-like) and DAAM (Dishevelled-associated activator of morphogenesis) (Campellone and Welch., 2010) and the genes of these formins are found in the starfish genome also. When the protein sequences are compared, DAD of ApDia shows low similarity to DAD of these formins except DAAM, but in literature DAAM is not

reported to be involved in cytokinesis.

PBE was also rescued when oocytes were injected with GST-ApDia-GBD/DID or GFP-mDia-GBD/DID (Fig. 4-12A-C), which do not show any significant similarity to GBD/DID of other formins. All together these observations suggest that GST-DAD and GST-GBD peptides target Dia, interfere with the intramolecular DID-DAD interaction and specifically activates endogenous ApDia, but not other formins.

4.2.6 PBE rescue by ApDia-fsDAD

To further verify that activation of ApDia, following injection of GST-ApDia-DAD, is responsible for the restoration of PBE in MAPK-inhibited oocytes, a mutant with two frame-shift mutations was used. These mutations were a single nucleotide insertion and a single nucleotide deletion at the beginning and end of the DAD, respectively, so that the sequence was changed from DQAG**VMD**N**L**LE**AL**QSGT**AF**NRGDKGGRKR to DQAGGWIIYWRHCRVVRPSTEGDKGGRKR (Fig. 4-13A). The ApDia-DAD core sequence is underlined and the residues essential for the interaction with DID are in bold (Nezami et al., 2010; Otomo et al., 2010). In this mutant, the C-terminal basic residues (double-underlined) are intact, which might be crucial for full ApDia activity (Gould et al., 2011). This mutant is called ApDia-frameshifted DAD (ApDia-fsDAD) and is expected to be constitutively active.

Immature oocytes were injected with HA-GFP2-ApDia-fsDAD mRNA. After 5 hours, the oocytes were induced for meiotic maturation in the presence of 5 μM U0126. Live-cell imaging of maturing oocytes showed that, although fine localization of GFP2-ApDia was not fully recovered, GFP2-ApDia was enriched at cleavage furrow (Fig. 4-13B, 64–71 min, arrowheads), the cleavage furrow closed and the first PBE was restored in these oocytes (Fig. 4-13B, 64–77 min) after which the oocytes entered parthenogenesis (Fig. 4-13B, 150 min). To further confirm the involvement of actin nucleating activity of ApDia in the rescue of PBE, the I699 residue of ApDia was mutated to alanine (homologous to the I704A mutation in mouse mDia2) (see Fig. 4-6, red arrow) to generate ApDia that cannot bind and nucleate actin filaments

(Bartolini et al., 2008). In the presence of U0126, expression of this mutant did not rescue the first PBE, whereas HA-GFP2-ApDia-fsDAD did, despite both proteins being expressed at a similar level (Fig. 4-13C and D). These data indicate that the FH2 domain of ApDia functions in PBE and that activation of ApDia by relief of the DID-DAD interaction is regulated by MAPK.

A

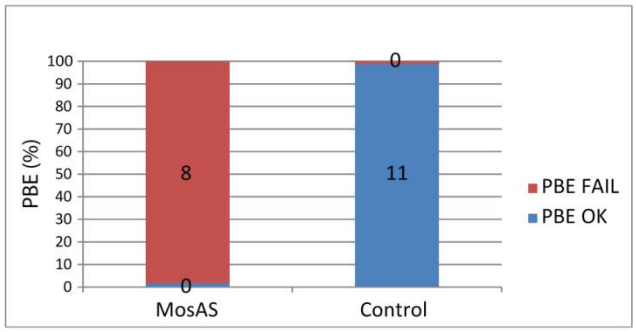
100
90
80
70
60
50
40
30
20
10
0
PBE (%)
8
0
0
11
MosAS
Control
PBE FAIL
PBE OK

B

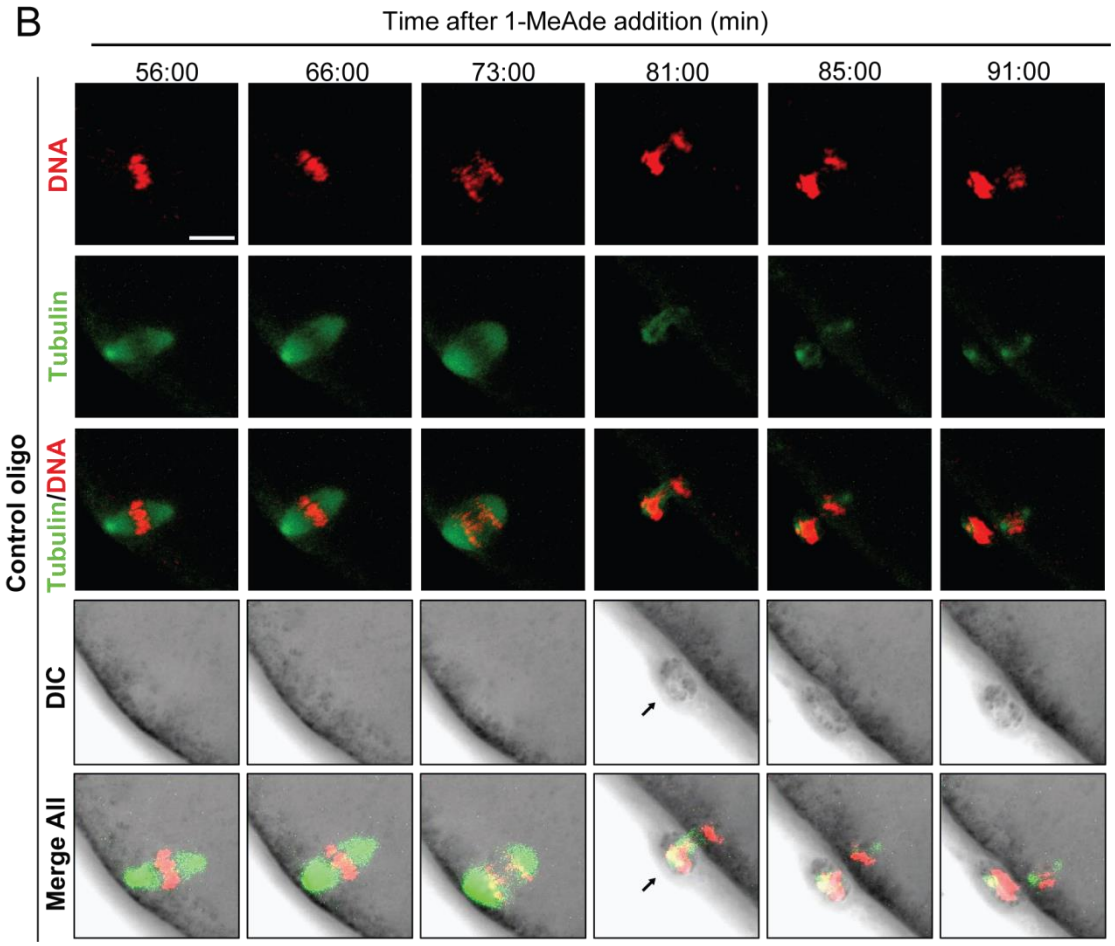
Time after 1-MeAde addition (min)
56:00
66:00
73:00
81:00
85:00
91:00
Control oligo
DNA
Tubulin
Tubulin/DNA
DIC
Merge All

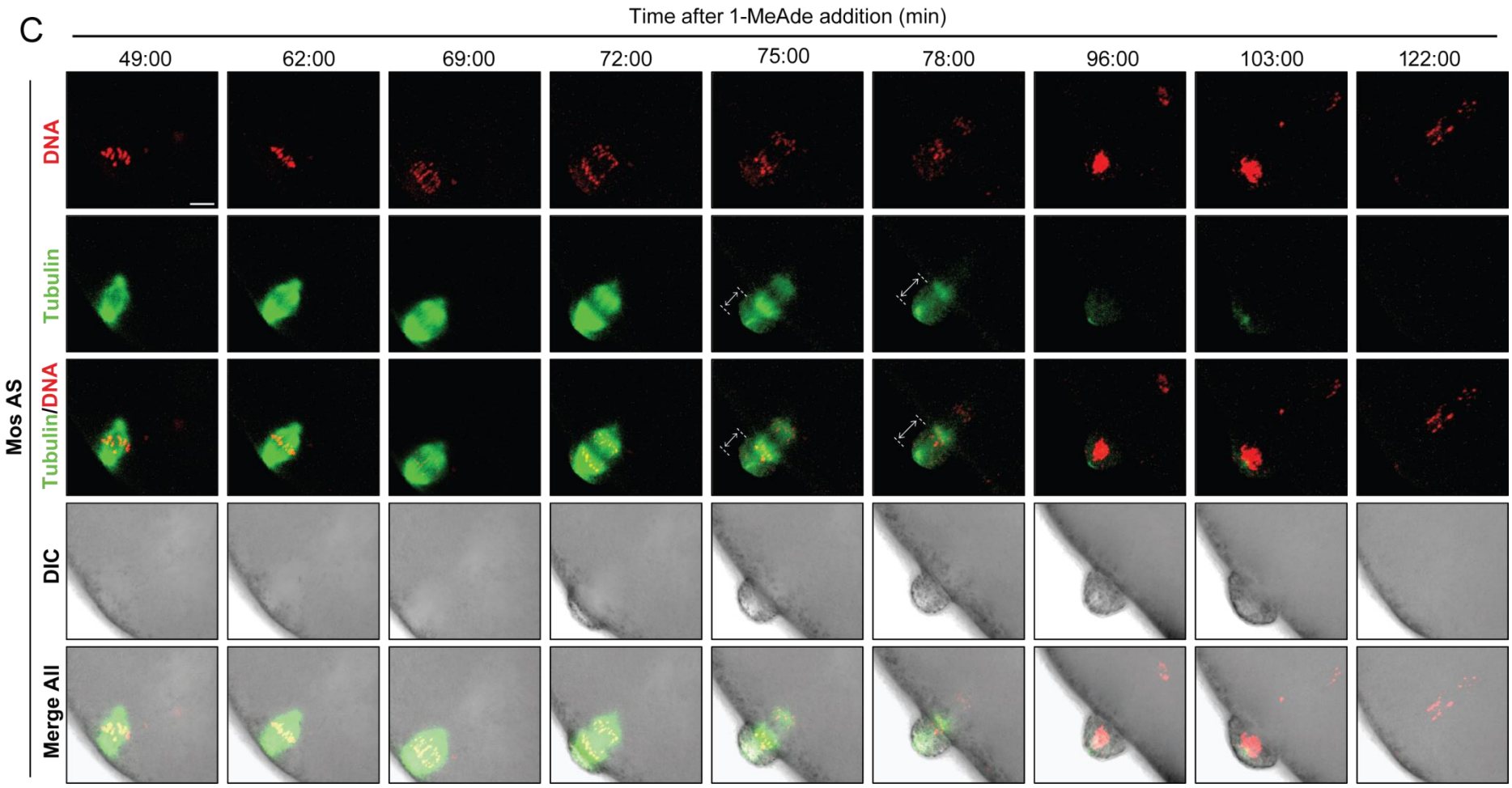
C
Time after 1-MeAde addition (min)
49:00
62:00
69:00
72:00
75:00
78:00
96:00
103:00
122:00
Mos AS
DNA
Tubulin
Tubulin/DNA
DIC
Merge All

Fig. 4-1. Spindle attachment at the cortex and cleavage furrow closure during PBE are regulated by Mos. (A) Fully-grown immature oocytes were injected with control oligonucleotide or MosAS, and then PBE was monitored 2.5 hours after inducing meiotic maturation. Numbers inside the bars indicate number of oocytes with or without PBE. **(B-C)** To monitor the spindle during the first PBE, immature oocytes were injected with HiLyte-488-labeled tubulin and Alexa-568-labeled histone H1 together with control oligonucleotide (B) or MosAS (C), and then oocytes were treated with 1-MeAde. During maturation, Z-section images of the PBE area were taken at approximately 1 minute intervals with a confocal microscope equipped with a 40× water lens. Z-sections were then piled to represent single time points and movies were prepared with these piled images. Representative images are shown. Scale bar, 10 μm. Black arrow (B) indicates protrusion; double sided arrow (C) indicates distance of spindle from cortex. Note that the spindle pole distal to cortex is out of focus in (C, 78 min).

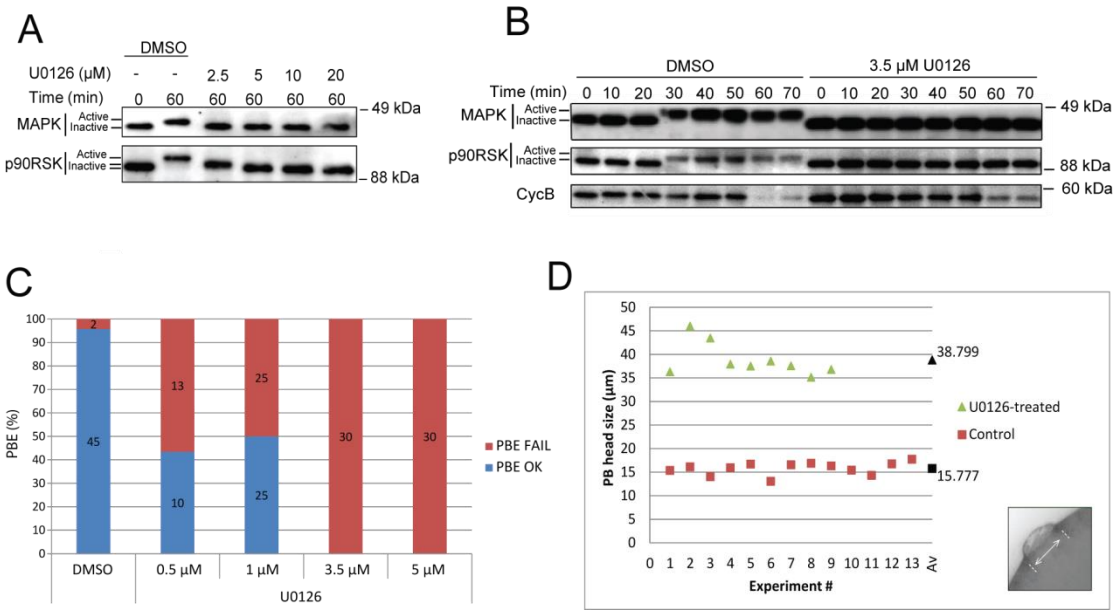

Fig. 4-2. MAPK activity is required for PBE (A) Fully-grown immature oocytes were treated with DMSO (control) or indicated concentrations of U0126, and then maturation was induced with 1-MeAde. Oocytes were collected at 60 min after maturation induction and activities of MAPK and Rsk were examined by western blotting. **(B)** Oocytes were collected at 10 min intervals after 1-MeAde treatment in the presence or absence of 3.5 3.5 μM U0126 and western blotting was performed for MAPK and p90Rsk. **(C)** Oocytes that are maturated in the presence of indicated concentrations of U0126 were examined for PBE 2.5 hours after 1-MeAde treatment. Numbers inside the bars indicate number of oocytes with or without PBE. **(D)** Size of the protrusion (see inset) was measured in control oocytes and U0126-treated oocytes. Each colored triangle or square indicate individual experiments, black triangle and black square indicates average of 9 control and 13 U0126-treatment experiments respectively.

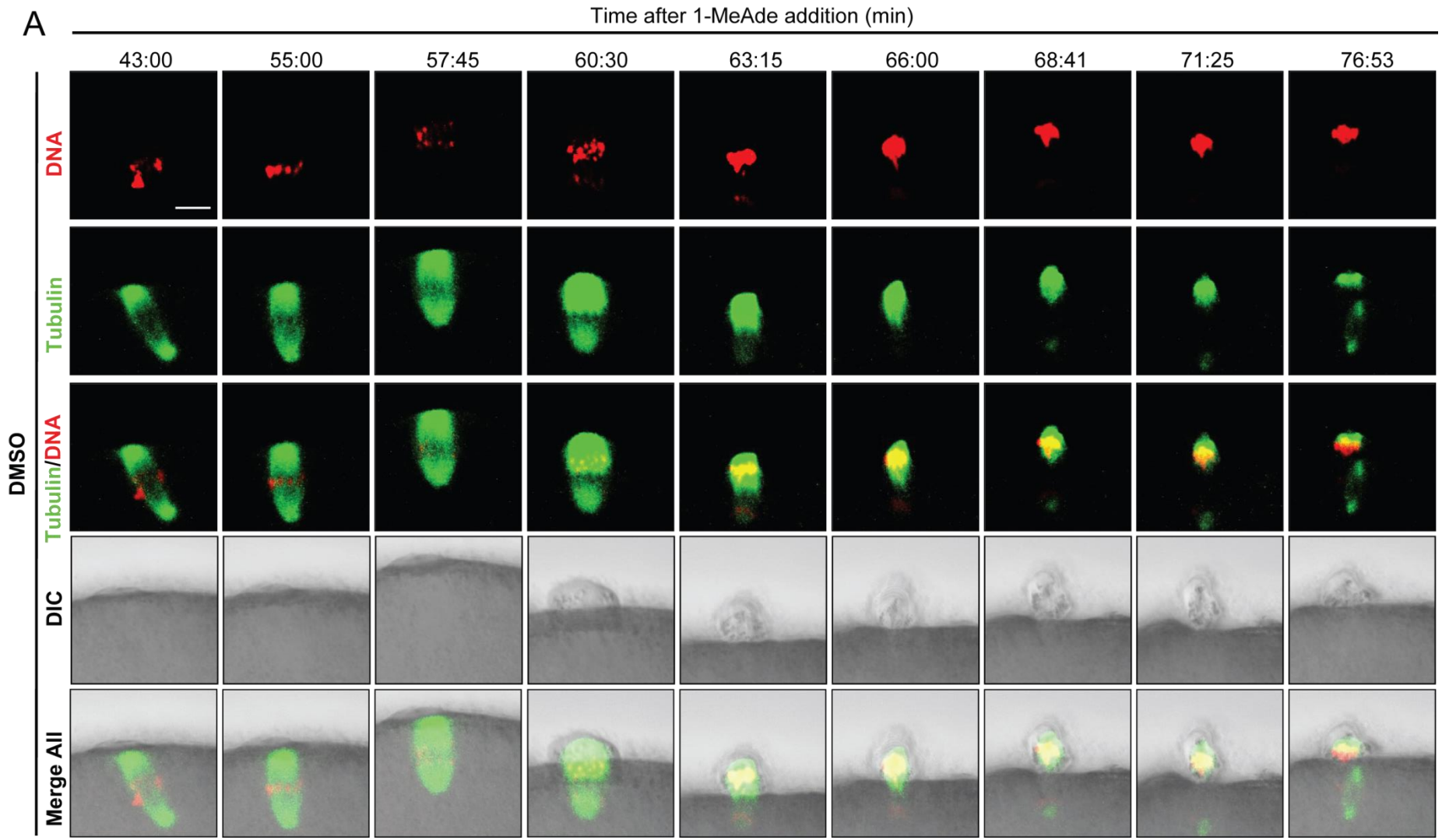
A
Time after 1-MeAde addition (min)
43:00
55:00
57:45
60:30
63:15
66:00
68:41
71:25
76:53
DMSO
DNA
Tubulin
Tubulin/DNA
DIC
Merge All

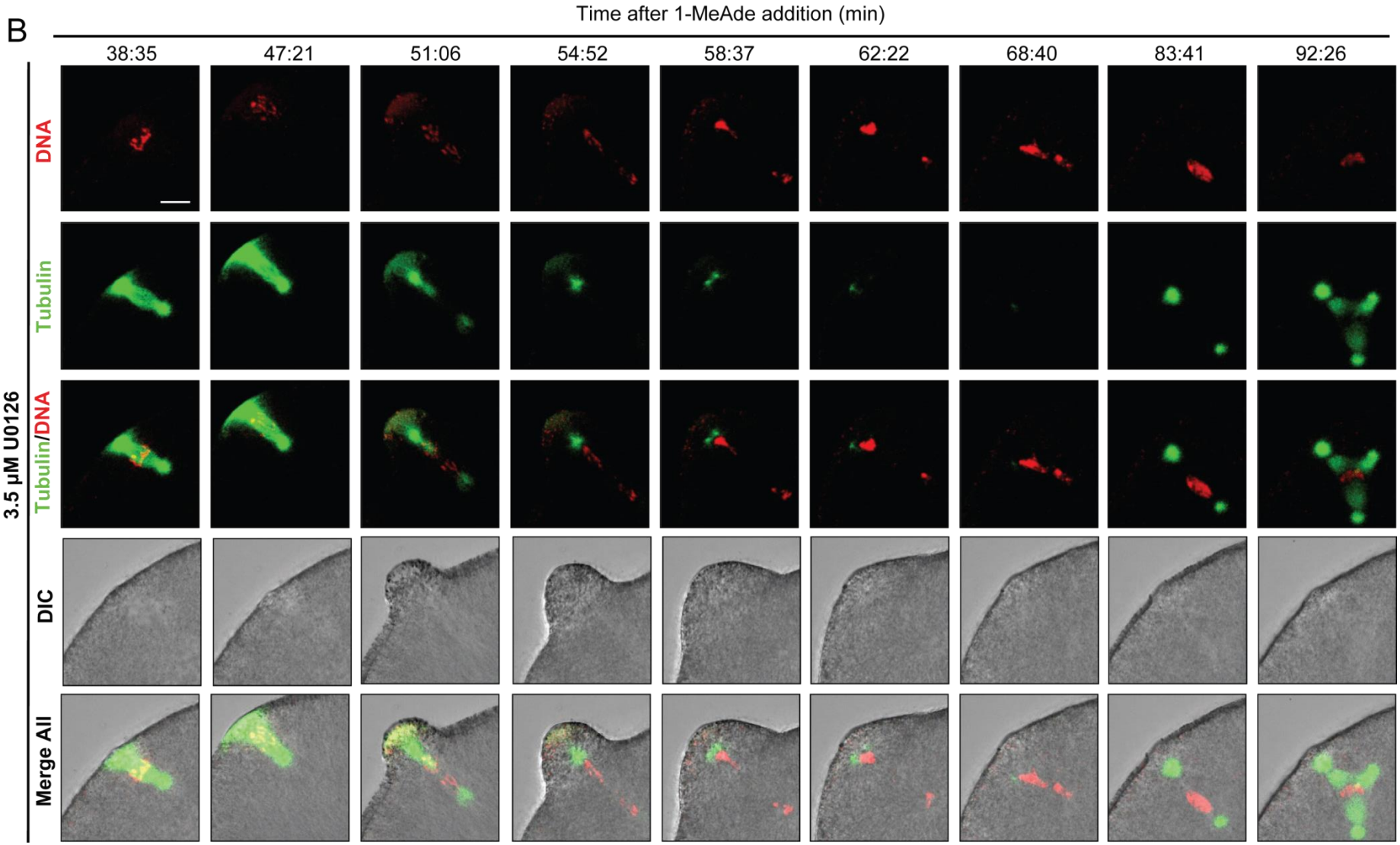
B
Time after 1-MeAde addition (min)
38:35
47:21
51:06
54:52
58:37
62:22
68:40
83:41
92:26
3.5 μM U0126
DNA
Tubulin
Tubulin/DNA
DIC
Merge All

Fig. 4-3. MAPK activity is required for tight spindle attachment to cortex during PBE and cleavage furrow closure. Immature oocytes were injected with HiLyte-488-labeled tubulin and Alexa-568-labeled histone H1. Then, spindle dynamics were observed by live-cell imaging in maturing oocytes in the presence of DMSO (A) or 3.5 μM U0126 (B). Scale bar, 10 μm.

A

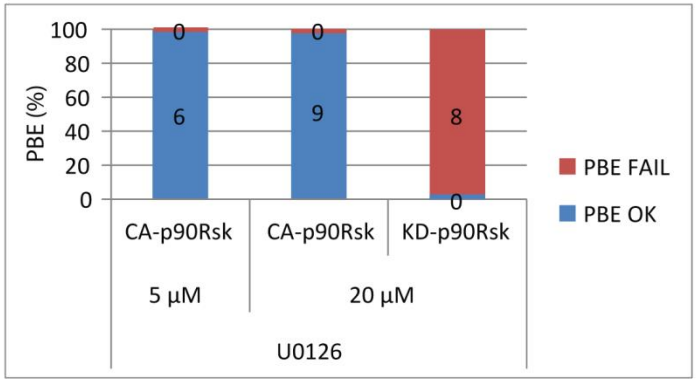
100
80
60
40
20
0
PBE (%)
0
6
0
9
8
0
PBE FAIL
PBE OK
CA-p90Rsk
CA-p90Rsk
KD-p90Rsk
5 µM
20 µM
U0126

B

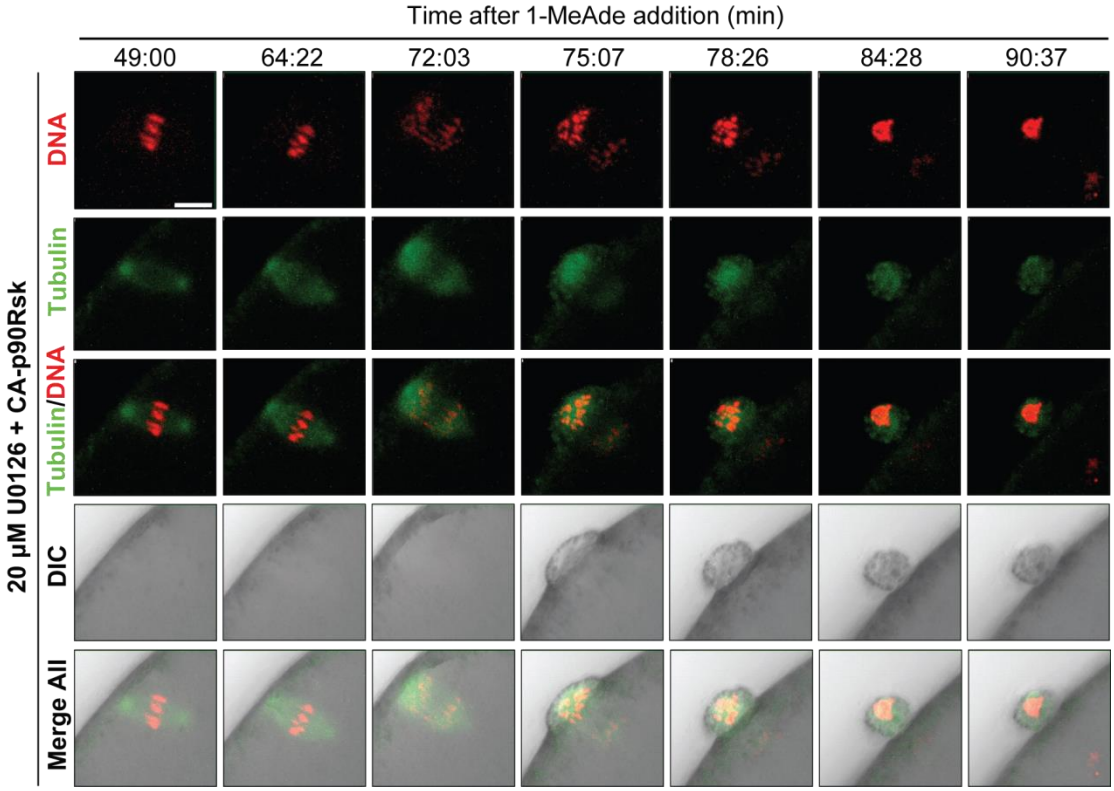
Time after 1-MeAde addition (min)
49:00
64:22
72:03
75:07
78:26
84:28
90:37
20 µM U0126 + CA-p90Rsk
DNA
Tubulin
Tubulin/DNA
DIC
Merge All

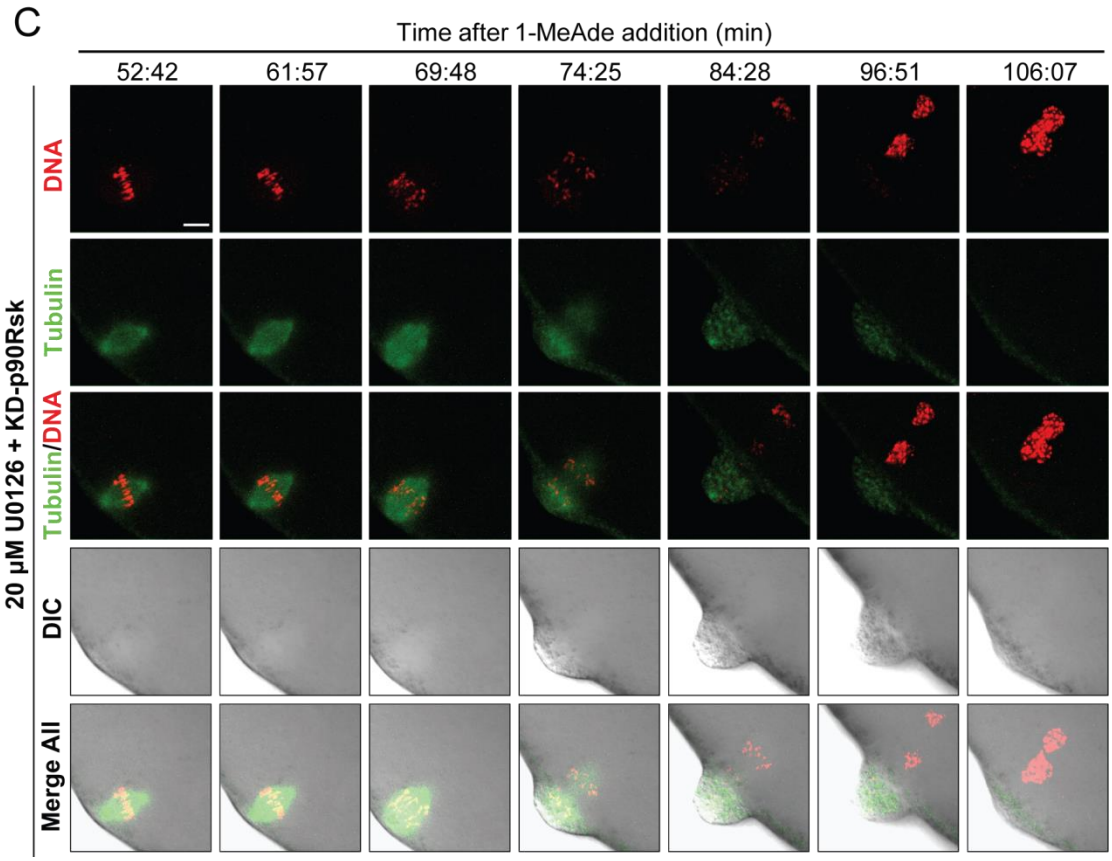

Fig.4-4. Constitutively active p90Rsk rescues PBE in MAPK-inactivated oocytes. (A) Fully-grown immature oocytes were injected with 100 pg CA-p90Rsk or 100 pg KD-p90Rsk and maturation was induced in the presence of indicated concentrations of U0126, and then PBE was monitored 2.5 hours after inducing meiotic maturation. Numbers inside the bars indicate number of oocytes with or without PBE. All oocytes injected with CA-p90Rsk succeeded in PBE whereas KD-p90Rsk injected oocytes did not. **(B-C)** Immature oocytes were injected as in Fig. 4-3A together with 100 pg CA-p90Rsk (B) or 100 pg KD-p90Rsk (C), and then spindle dynamics were observed by live-cell imaging in maturing oocytes in the presence of 20 μM U0126. Scale bar, 10 μm.

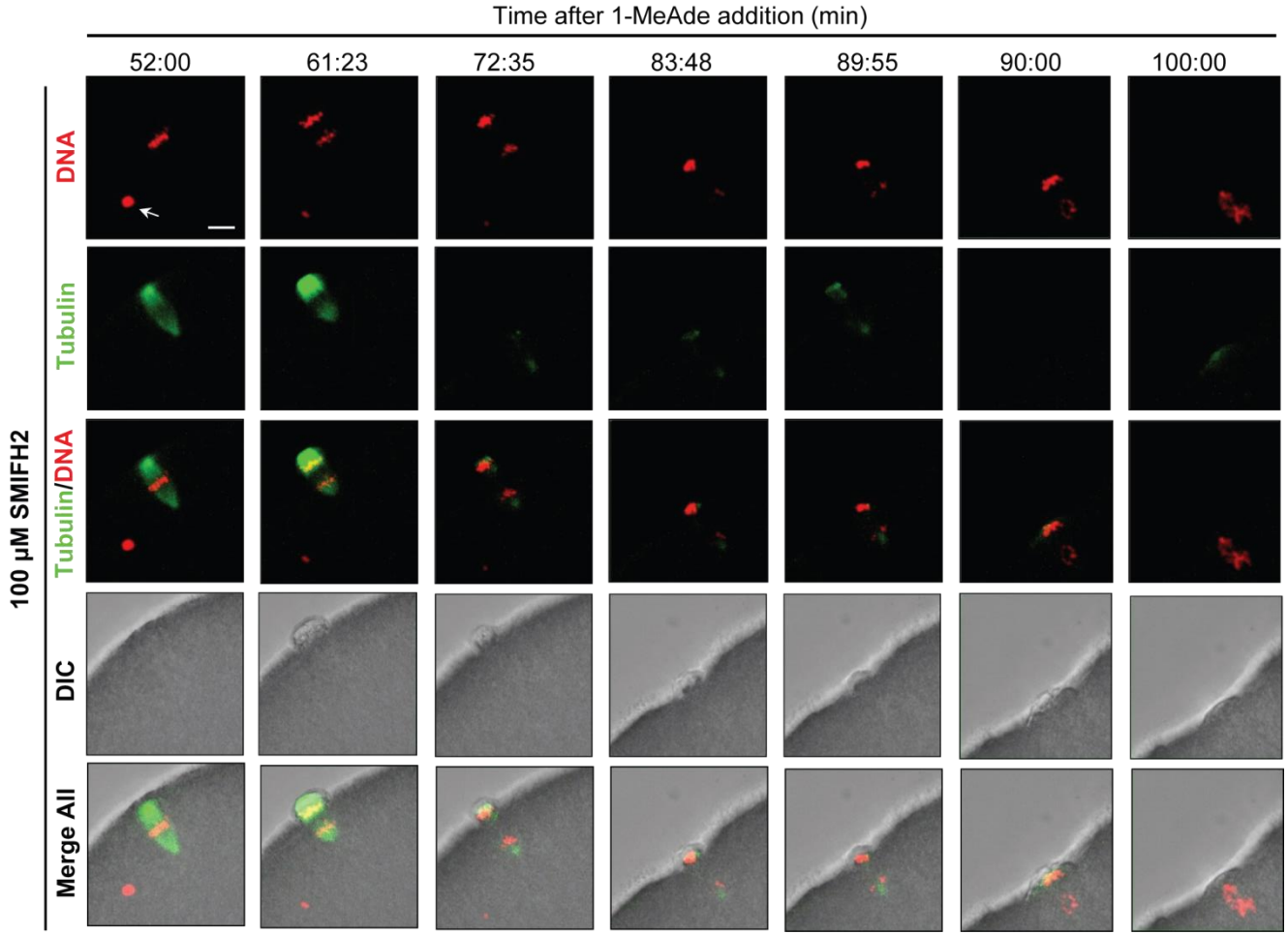

Fig. 4-5. FH2 domain activity of formins is required for PBE. Immature oocytes were injected as described in Fig. 4-2A and then treated with 100 μM SMIFH2 after GVBD (at 30 min after 1-MeAde treatment).Scale bar, 10 μm.

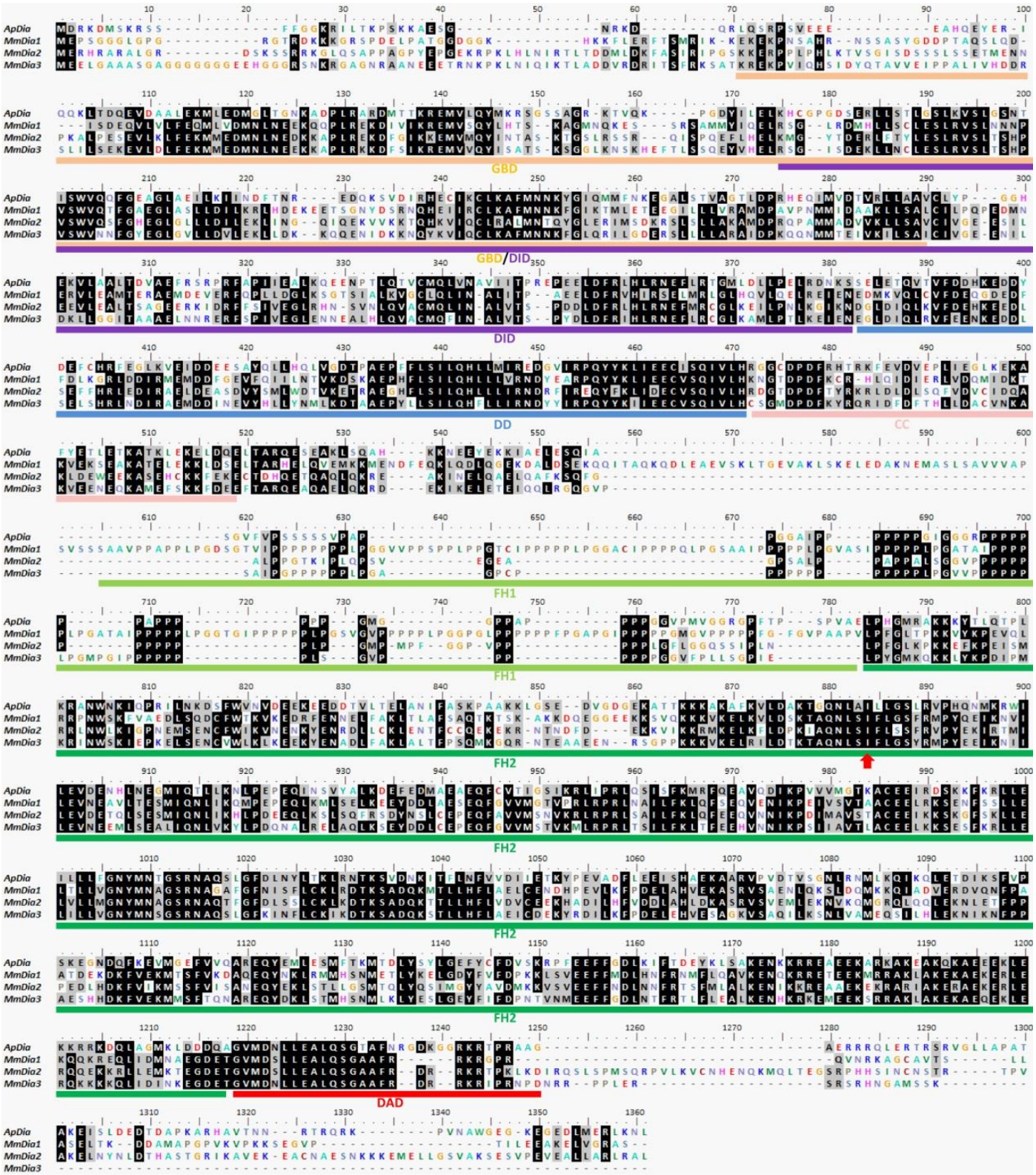
ApDia
MmDia1
MmDia2
MmDia3
GBD
GBD/DID
DID
DD
CC
FH1
FH1
FH2
FH2
FH2
DAD

Fig. 4-6. Cloning of ApDia. Deduced amino acid sequence of ApDia was aligned with those of mouse Dia using the multiple cluster alignment function of the BioEdit Sequence Alignment Editor program. Colored lines indicate the domains, the names of which are provided beneath each line as follows: GBD, GTPase-binding domain; DID, DAD-interacting domain; DD, dimerization domain; CC, coiled coil; FH1, formin homology 1 domain; FH2, formin homology 2 domain; DAD, Dia autoregulatory domain. The arrow indicates the I704 residue which is required for actin binding and nucleation activity of mDia2. Of the ApDia residues, 34%, 36% and 37% are identical to and 50%, 55% and 55% are similar to those of mDia1, mDia2 and mDia3 respectively, indicating that ApDia represents all mDia proteins as a single protein. Detailed investigation of ApDia further supports this idea that ApDia shares identity with different mDia proteins at different residues even in the same regions (compare D1047, E1050, K1052, and YPEV1053–1056 or M1210, K1211, and N1223. Numbers indicate positions according to the ruler of the alignment). Accession number of ApDia; KC701713.

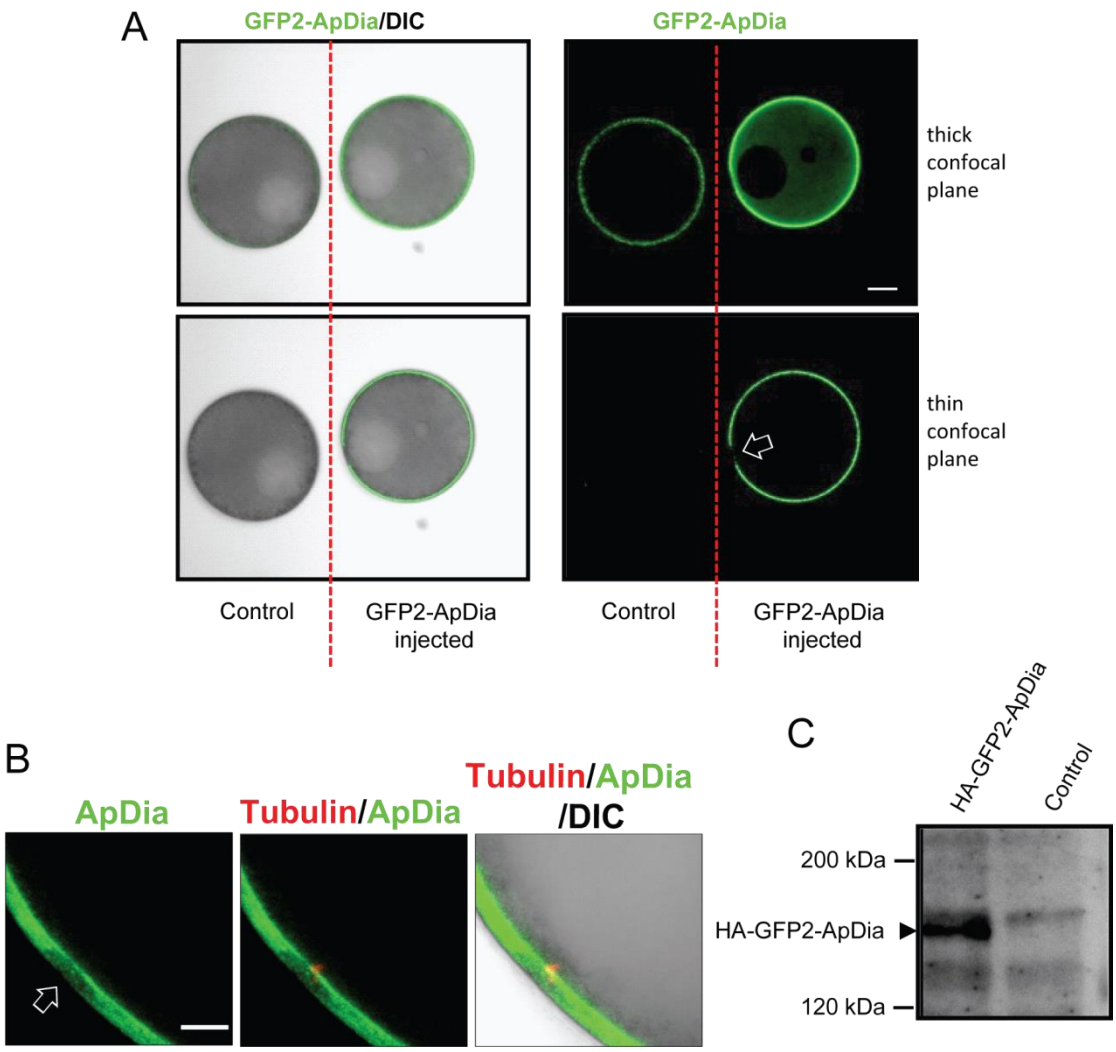

Fig. 4-7. Immature oocytes have a distinct pattern of ApDia localization at the animal pole. (A) Immature oocytes were injected with rhodamine-labeled tubulin and HA-GFP2-ApDia mRNA. Five hours later, GFP2-ApDia fluorescence was examined to determine the expression and localization of ApDia. A non-injected control oocyte is shown on the left. Upper and lower panels show thick and thin focal planes, respectively. **(B)** 24 Z-section images spanning animal pole shows GFP2-Dia absent region in 3D. **(C)** Western blotting with an anti-HA antibody was performed on samples prepared from 10 oocytes expressing HA-GFP2-ApDia. Arrow (A) indicates a nucleolus artifact, open arrows (A, B) indicate absence of ApDia. Scale bar in (A) is 50 µm. Scale bar in (B) is 10 µm.

DMSO
Merge All
DIC
Tubulin/ApDia
Tubulin
ApDia
Time after 1-MeAde addition (min)
52:13
59:39
60:23
61:08
61:52
63:21
65:35
67:49

Fig. 4-8. ApDia localizes at the cleavage furrow as a ring-shape. HA-GFP2-ApDia expressing oocytes in Fig 4-7A-B were observed by live-cell imaging during maturation in the presence of DMSO. After spindle attachment to the cortex, GFP2-ApDia was absent from the cortex of the protrusion and concentrated at cleavage furrow in control oocytes. Arrowheads indicate ApDia localization at cleavage furrow. Scale bar, 10 μm.

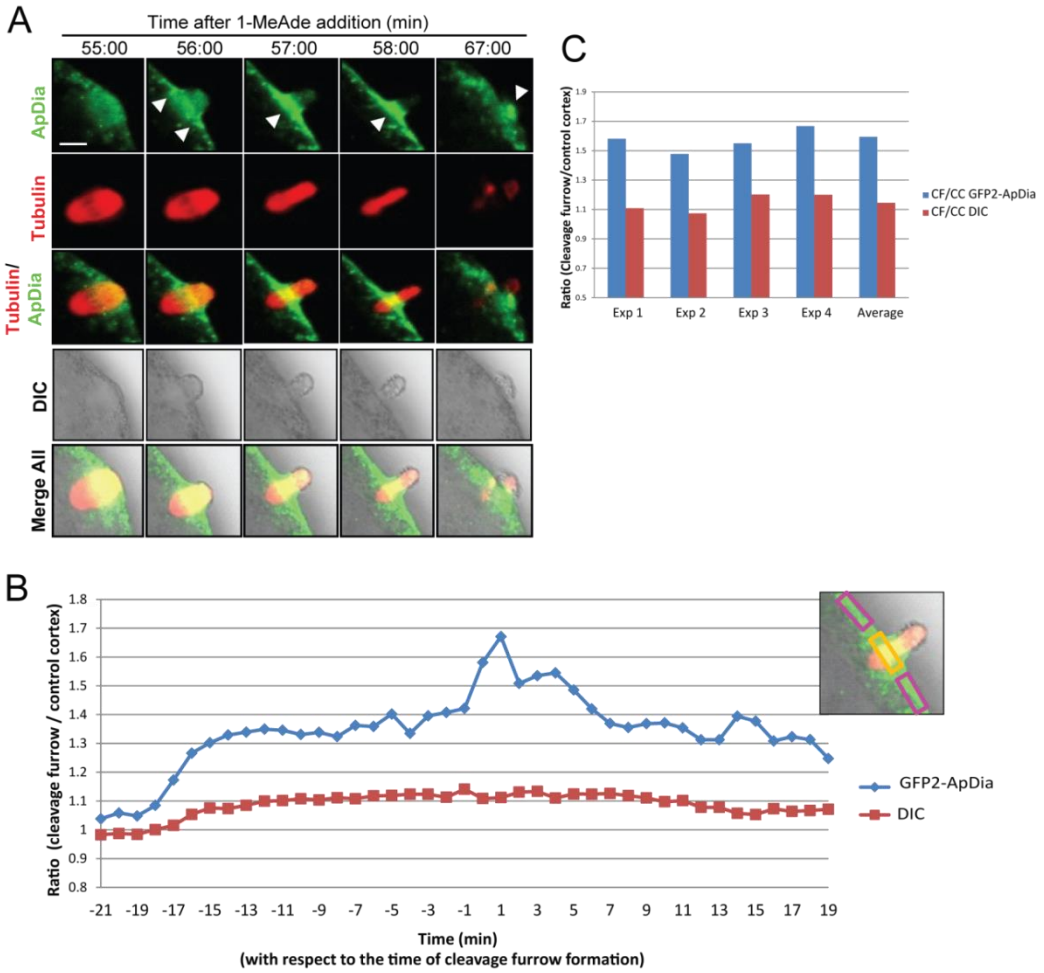

Fig. 4-9. GFP2-ApDia enrichment at cleavage furrow. (A) HA-GFP2-ApDia expressing oocytes were treated with DMSO and then maturation was induced. Representative images of GFP2-ApDia localization at cleavage furrow are shown. Arrowheads indicate GFP2-ApDia at the furrow. (B) HA-GFP2-ApDia enrichment at the furrow region was quantified as following; GFP2 and DIC signals at clevage furrow (CF) region and at two control cortex (CC) regions (orange and purple rectangles respectively in the inset) with same surface area were quantified. Signals at CF were divided by the average of two CC regions. -17 min corresponds to spindle attachment to the cortex. (C) GFP2-ApDia enrichment at the time of CF formation was analyzed in 4 different experiments; in average GFP2-ApDia gets enriched 1.67 times at the CF.

3.5 μM U0126
Merge All
DIC
Tubulin/ApDia
Tubulin
ApDia
Time after 1-MeAde addition (min)
60:37
63:49
66:58
71:15
81:54
88:15
95:40
106:16

Fig. 4-10. Fine pattern of ApDia localization at the cleavage furrow is controlled by MAPK activity. HA-GFP2-ApDia expressing oocytes were observed by live-cell imaging during maturation in the presence 3.5 μM U0126. After spindle attachment to the cortex, although GFP2-ApDia was absent from the cortex of the protrusion in DMSO treatments, in U0126-treated oocytes, GFP2-ApDia absence at the protrusion was lost and GFP2-ApDia localized all around the protrusion with higher signals at possible cleavage furrow regions. Arrowheads indicate ApDia localization at possible prospective cleavage furrow. Scale bar, 10 μm.

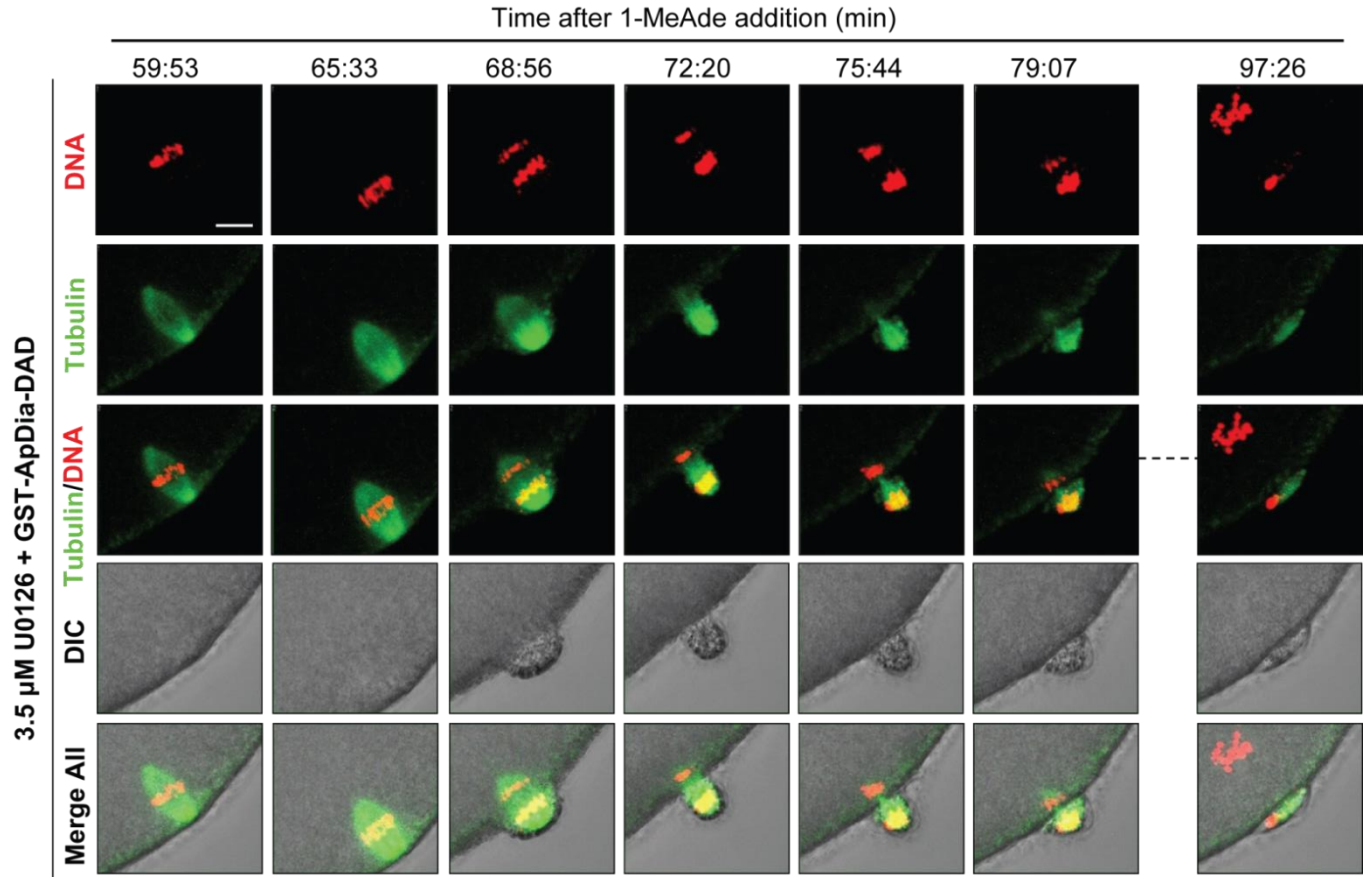

Fig. 4-11. Activation of endogenous ApDia by injection of GST-ApDia-DAD rescues PBE in U0126-treated oocytes. Immature oocytes were injected as described in Fig. 4-2E together with 2.4 pg of GST-ApDia-DAD, and then spindle dynamics were observed by live-cell imaging in maturing oocytes in the presence of 3.5 μM U0126.

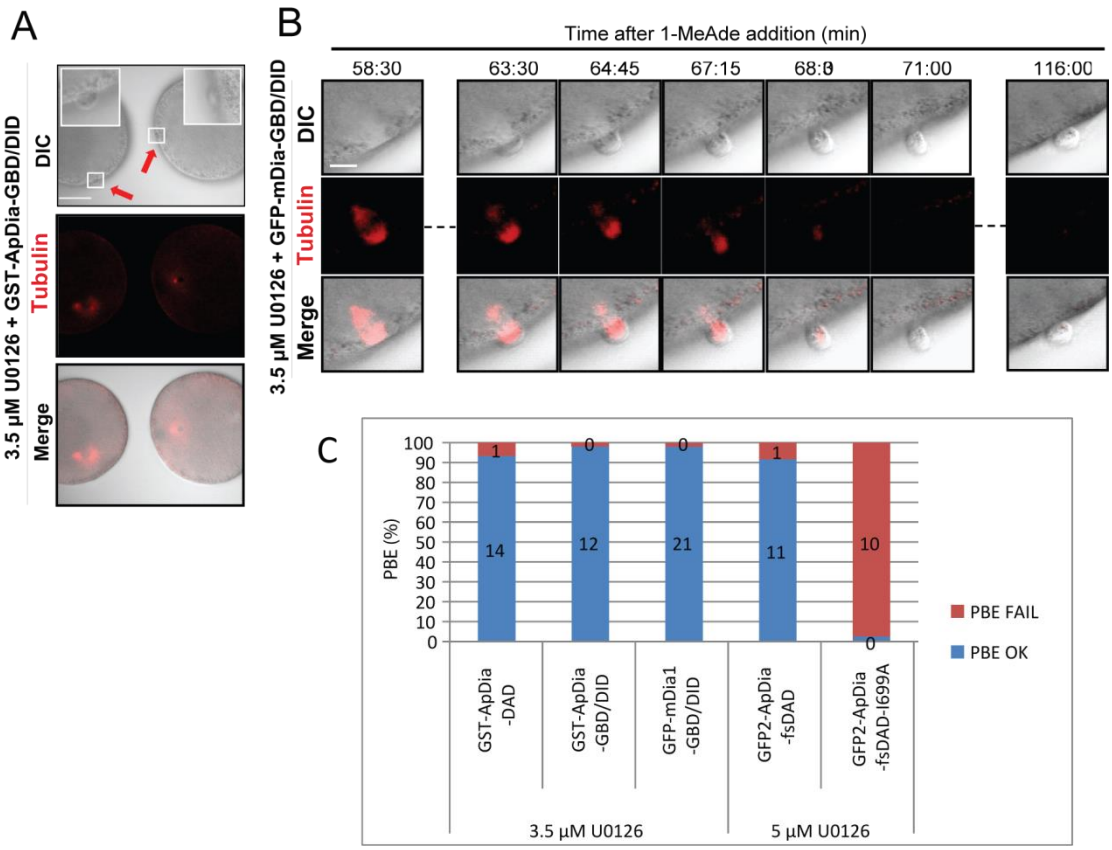

Fig. 4-12. Activation of endogenous ApDia by injection of GST-ApDia-GBD/DID or GFP-mDia-GBD/DID rescues PBE in U0126-treated oocytes. (A) Oocytes were injected with rhodamine-labeled tubulin (red) and GST-ApDia-GBD/DID, treated with 3.5 μM U0126, and then treated with 1-MeAde to induce maturation. The images shown here are of two oocytes which entered parthenogenesis but retains PB. Note that the confocal planes of the polar bodies and the tubulin asters are different. Scale bar, 50 μm. (B) Oocytes were injected with rhodamine-labeled tubulin (red) and GFP-mDia1-GBD/DID (green is not shown for simplicity), and then treated as in (A). Images were taken at 30 sec intervals during the first PBE. Scale bar, 10 μm. (C) Statistical data showing PBE failure or success in oocytes injected with the indicated proteins or mRNAs. Numbers inside the bars indicate number of oocytes.

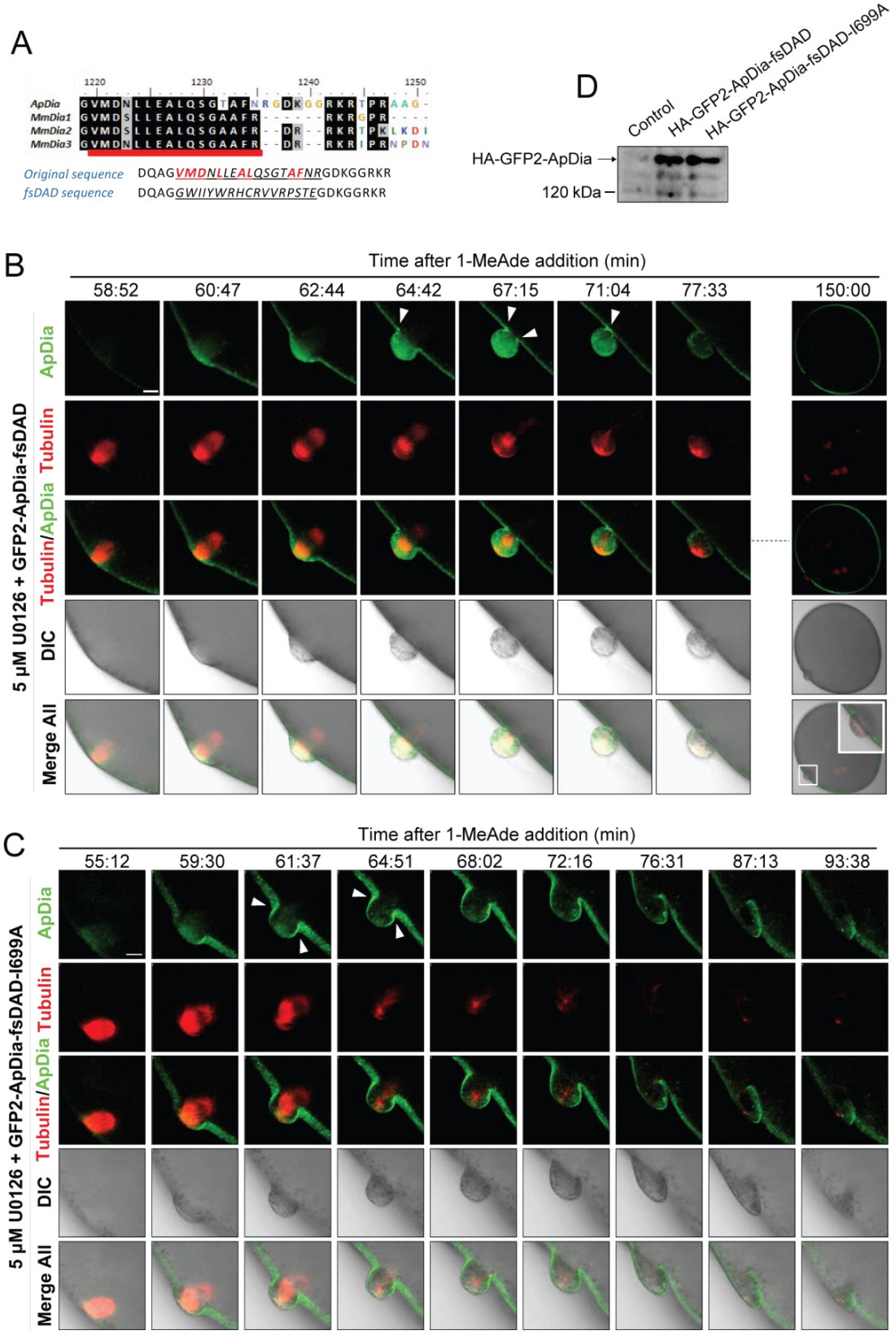
A
1220
1230
1240
1250
ApDia
MmDia1
MmDia2
MmDia3
Original sequence DQAGVMDNLLEALQSGTAFNRGDKGGRKRTPRAAG
fsDAD sequence DQAGGWIIYWRHCRVVRPSTEGDKGGRKR
D
Control
HA-GFP2-ApDia-fsDAD
HA-GFP2-ApDia-fsDAD-I699A
HA-GFP2-ApDia
120 kDa
B
Time after 1-MeAde addition (min)
58:52
60:47
62:44
64:42
67:15
71:04
77:33
150:00
5 µM U0126 + GFP2-ApDia-fsDAD
ApDia
Tubulin
Tubulin/ApDia
DIC
Merge All
C
Time after 1-MeAde addition (min)
55:12
59:30
61:37
64:51
68:02
72:16
76:31
87:13
93:38
5 µM U0126 + GFP2-ApDia-fsDAD-I699A
ApDia
Tubulin
Tubulin/ApDia
DIC
Merge All

Fig. 4-13. Expression of constitutively active ApDia rescues PBE in U0126-treated oocytes. (A) The highly conserved DAD region (underlined) of ApDia was mutated into a non-related sequence to generate HA-GFP2-ApDia-fsDAD. **(B, C)** HA-GFP2-ApDia-fsDAD (B) or HA-GFP2-ApDia-fsDAD I699A (C) mRNA was injected into immature oocytes, and then these oocytes were observed by live-cell imaging during maturation in the presence of 5 μM U0126. **(D)** Western blotting with an anti-HA antibody was performed on samples prepared from 10 of the oocytes described in (C) and (D). PBE was rescued in (A) and (C) but not in (D). Inset in (C) indicates that PB is preserved even after parthenogenesis. Arrowheads indicate ApDia localization at cleavage furrow Scale bar, 10 μm.

5. DISCUSSION

In this study, I show that the Mos-MAPK pathway regulates the maintenance of tight spindle attachment to the cortex, proper chromosome separation and cleavage furrow closure during PBE, and that these are mediated by Dia in starfish oocytes. ApDia localization was shown for the first time at cleavage furrow during PBE. My data suggest that fine adjustment of Dia localization and its activation are regulated by the Mos-MAPK pathway (Fig. 5-1).

First of all, live-cell imaging enabled me to observe fate of single oocytes during maturation in terms of spindle dynamics and PBE. If oocyte fixation method is used, as used by many others in PBE studies in different organisms, one cannot understand in the fixed samples whether a single oocyte retains polar body or there is an occasional polar body like structure caused by uncontrolled contractions. By using live-cell imaging, I have avoided this, and observed that inhibition of the Mos-MAPK pathway causes several defects which results in PBE failure.

5.1 Roles of the Mos-MAPK pathway during PBE

My data indicate that although MAPK is activated at the time of GVBD, it has no visible effect on the formation of spindle or its slight but significant movement to the oocyte cortex. Moreover, spindle attachment to cortex and spindle rotation was also not affected by the inhibition of Mos synthesis or MAPK activity. While spindle rotation could be explained by the fact that MAPK has no effect on Aurora activity (Abe et al., 2011), no involvement of MAPK in spindle movement seems in contrary to a very recent publication (Chaigne et al., 2013) which shows MAPK activity involvement in spindle movement to cortex by regulating Arp2/3 activity via Wasp phosphorylation in mouse

oocytes. It is possible that the mechanisms involved in spindle movement to cortex are different when the spindle is in close proximity to the cortex and when the spindle is at the center of the oocytes; when the spindle is at the center, MAPK activity might be regulating spindle movement to cortex via Arp2/3 dependent mechanism, but when spindle is near the cortex, other actin dependent mechanisms that are independent of MAPK activity might be functioning. Another possibility is that, astral microtubule fibers, that are too short to be involved in spindle movement when spindle is far from cortex, might be having significant effects on spindle movement when the spindle is close to the cortex. Indeed, short microtubule fibers are involved in spindle attachment and polarized spindle localization during unequal cell division of the budding yeast (McNally, 2013).

My data indicate that the Mos-MAPK pathway is involved in PBE in starfish oocytes (Fig. 5-1). Rescue of PBE by CA-p90Rsk suggests that p90Rsk downstream of MAPK is also involved in PBE. As mentioned earlier, previous reports showed that Mos-KO mouse oocytes succeeded in PBE but inhibition of the Mos-MAPK pathway activity at GV-phase either with MosAS injection or U0126-treatment prevents PBE in pig, mouse and cnidarian oocytes. My results are in accordance with the latter case. Although literature data cannot explain why Mos-KO mouse oocytes emit PB, they indicate that the Mos-MAPK pathway is involved in PBE not only in starfish oocytes but also in other organisms. Interestingly, my unshown data shows that starfish oocytes which were not fully-grown, emitted large PBs in both MosAS injected and 20 μM U0126-treated oocytes, suggesting that starfish oocytes respond differently in different growth phases which might be attributed to expression

levels of certain proteins in positive- or negative-feedback loops of regulatory systems that are involved in PBE. A simple mechanism that could be imagined is as follows; a substrate of the Mos-MAPK pathway that is essential for the PBE is the substrate of another kinase (X-kinase) which has kinase activity before PBE but loses its activity at the time of PBE. Thus, activation of the substrate by the X-kinase will take place before PBE even in the absence of MAPK activity. If a phosphatase that dephosphorylates the substrate is not accumulated sufficiently in the not fully-grown oocytes, in the absence of MAPK activity (when oocytes treated with U0126 or injected with MosAS), the substrate will remain active due to previous phosphorylation by the X-kinase and will perform its function in PBE.

5.2 Localization of ApDia

It was observed that GFP2-ApDia localized strongly at the cortex of immature oocytes, leaving a hole like empty region at the animal pole. The centrosomes are located close to this Dia-absent region in immature oocytes and during maturation the polar bodies are emitted at this region. Since artificial arrangements in the positioning of GV alters the position of PBE (Matsuura and Chiba, 2004), it is plausible that positioning of the Dia absent region is also GV-dependent. Contents of GV (mainly chromosomes) were previously shown to regulate cortical organization of actin via Ran-gradient and Rac1 activity (Deng et al., 2007; Halet and Carol, 2007). In this context, it would be interesting to analyze whether regulation of localization pattern of Dia involves signals of Ran-gradient or small-GTPases that are originating from GV. Very strong F-actin signals at the cortex were observed by using an F-actin probe (GFP-UtrCH) in oocytes of starfish and mouse (Mori et al., 2011;

Azoury et al., 2011; Chaigne et al., 2013). In connection with this, localization of Dia at the cortex might be responsible for the nucleation of F-actin at the cortex which might account for the rigidity of oocyte cortex.

During PBE, GFP2-ApDia was enriched at the cleavage furrow and formed a ring around the spindle. It was previously shown that, three straight F-actin nucleators, Formin-2, Spire1 and Spire2, are localized at cleavage furrow and required for PBE in mouse oocytes (Dumont et al., 2007; Campellone and Welch, 2010; Pfender et al., 2011). DNA sequences coding these proteins are present in starfish genome also and they are possibly functioning in starfish oocytes. Here, I am adding a new F-actin nucleator, Dia, that is required for PBE, but different from others; its localization and activation are under the regulation of the Mos-MAPK pathway. Localizing at the same region and functioning in the same process suggest that these F-actin nucleating proteins are functioning coordinately in PBE. Although spire family and Formin-2 are known to interact directly and function together (Pfender et al., 2011; Vizcarra et al., 2011; Kerkhoff et al., 2001), any interaction with Dia is yet to be discovered.

5.3 Regulation of ApDia activation and PBE

My results suggest that activities of the Mos-MAPK pathway are mediated by activation of Dia (Fig. 5-1). Although the precise mechanism is unknown, my preliminary data indicate that GST-DAD, but not GST-GBD/DID, is phosphorylated MAPK-dependently in oocyte extracts. Because of this, I suspect that a regulatory phosphorylation close to the DAD region is involved in the activation of ApDia. It is highly anticipated that, downstream of MAPK, p90Rsk is involved in the regulation of ApDia. But since there is no solid

evidence that ApDia is downstream of p90Rsk, currently I cannot rule out a possibility that p90Rsk and ApDia constitutes two parallel pathways downstream of MAPK, which of them are able to compensate each other`s activities. Moreover active-p90Rsk cannot directly phosphorylate DAD *in vitro* (data not shown), indicating that even if ApDia is downstream to p90Rsk, there should be at least another kinase which mediates DAD phosphorylation.

According to a previous study in starfish oocytes, inhibition of MAPK activity by U0126-treatment causes a decrease in Plk1 activity just before PBE (at 60 min after 1-MeAde treatment). Parallel with this report, according to the preliminary data of mine, in western blot analysis, Plk1 mobility showed differences in MAPK-active and MAPK-inactivated oocytes at around the time of PBE. As mentioned before, Plk1 is one of the key regulators for the localization and organization of the contractile ring in somatic cells. In starfish oocytes inhibition of Plk1 activity prevents PBE, but since inhibition of Plk1 causes loss of bipolar spindle arrangement at an earlier step before PBE, it is not clear whether Plk1 has any effect on cleavage furrow organization or not. According to my preliminary data, when Plk1 activity was inhibited with a chemical inhibitor at a timing so that it mimics the Plk1 activity loss of U0126-treated oocytes (loss of activity at about 60 min after 1-MeAde treatment), without the loss of bipolar spindle morphology, the oocytes failed to close their cleavage furrows. On the other hand, when GST-DAD was injected into immature oocytes, and then the Plk1 was inhibited 60 min after 1-MeAde treatment, oocytes succeeded in PBE. These data indicate that downstream of Mos-MAPK pathway, Plk1 might be mediating activation of Dia in starfish oocytes. The involvement of Dia could be through Ect2 activation, which in turn

activates RhoA, as in somatic cells or Plk1 could be the kinase that phosphorylates Dia near DAD at its C-terminus.

It is estimated that physiological concentrations of Rho may not fully activate Dia (Li and Higgs., 2003; Chesarone et al., 2010); therefore, it is possible that Rho and regulatory kinases act together to activate Diapahanous-related formins, and that in oocytes these kinases are regulated by MAPK. On the other hand, the possibility that activation of ApDia by the Mos-MAPK pathway involves Rho, as mentioned for Plk1, should also be in consideration. Actually, the loss of ApDia absent region at the protrusion in U0126-treated oocytes (Fig. 4-10) suggests that localization determinants are also disrupted. These localization determinants may include RhoA and Cdc42; as mentioned before, it is suggested that during PBE, Cdc42 drives dynamic F-actin via Arp2/3 complex which causes membrane protrusion, and RhoA drives stable F-actin which restricts this protrusion and exerts constriction at cleavage furrow (Zhang et al., 2008; Maddox et al., 2012). Activation of Arp2/3 during lamellipodia protrusion involves ERK-MAPK activity (Mendoza et al., 2011), and a recent study shows that the Mos-MAPK pathway triggers Arp2/3 activity during spindle movement to cortex (Chaigne et al., 2013), thus regulation of Arp2/3 during PBE by Mos-MAPK pathway is also possible. Moreover, the size of the membrane protrusion during PBE failure in MAPK-inhibited oocytes are ~2.5 larger than that of control oocytes (Fig. 4-2D), indicating that regulation of branched F-actin formation to a restricted area was not functioning properly when MAPK is inactivated. Since regulation of Arp2/3 and Dia might include involvement of Cdc42 and RhoA respectively, it would be interesting to examine whether active-RhoA and active-Cdc42 localizations

during PBE are regulated by the Mos-MAPK pathway or not (Fig. 5-2).

It should also be noted that, although localization pattern of ApDia is not totally rescued by the active-Dia (fsDAD mutant), cleavage furrow closure was accomplished and PBE was rescued. This suggests that activity of Dia may be more prominent than its localization. It should be also under consideration that we don`t know up to what extend GFP2-ApDia-fsDAD is overexpressed; since Dia forms dimers and there are inactive endogenous ApDia proteins in U0126-treated oocytes, it is possible that these endogenous inactive proteins alter localization of GFP2-ApDia-fsDAD. This notion can also explain why expression of GFP2-ApDia-fsDAD could not rescue spindle attachment defects observed in U0126-treated oocytes while activation of endogenous ApDia by GST-DAD or GST-GBD/DID could rescue all the defects caused by U0126-treatment.

In somatic cells, mDia3 is observed at kinetochore regions and shown to be important for the bipolar arrangement of chromosomes at the metaphase plate. In live cell imaging of this study, it was not possible to monitor Dia localization at the kinetochores due to technical reasons, but since ApDia represents all three isoforms of mammalian Dia, it is expected that ApDia functions in kinetochore organization also. Supporting this idea, when oocytes were injected with MosAS or treated with MAPK inhibitor, oocytes show chromosome separation defects, but when endogenous Dia is activated by GST-DAD injection in Mos- or MAPK-inhibited oocytes, chromosome separation defects were also recovered. This observation suggests that MAPK might be regulating Dia function at kinetochores also. Although, I did not monitor chromosome separation in ApDia-fsDAD expressing oocytes, parallel

with the above paragraph, like spindle attachment, it is possible that expression level of ApDia-fsDAD may not be sufficient for recovering chromosome separation defects.

5.4 What drives polar localization of cell division machinery?

Although many observations have been made on unequal cell division, one of the most fundamental questions remains unanswered. Almost all the molecules, discussed in this study and in other studies of PBE that are required for the cell division, are also involved in different steps of equal cell division; in both equal cell division and unequal cell division, CycB-Cdk1 is the major component of the M-phase regulating Plk1 and Aurora regulatory kinases, and then the downstream targets, small-GTPases and actin nucleators, form the contractile ring resulting in cell division. The question is; what is the uppermost regulatory element which drives these cell division machineries to function under the cortex during PBE instead of the center of the cell. The most possible candidates would be among the oocyte maturation specific cell cycle regulatory kinases, and although not clarified yet the Mos-MAPK pathway might perform such a role (Chaigne et all., 2013) (Fig. 5-3).

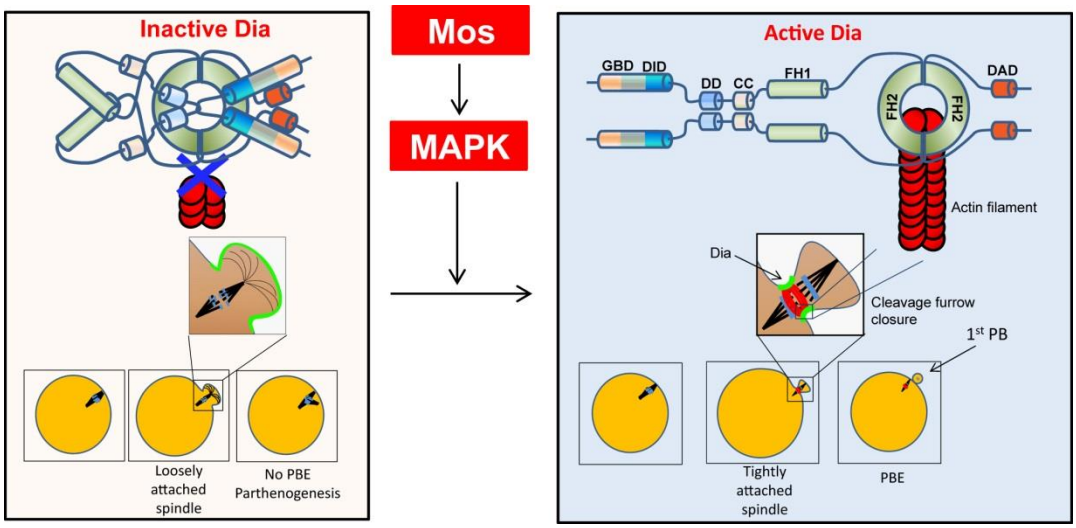

Fig. 5-1. Proposed model to explain how the Mos-MAPK pathway and ApDia mediate the first PBE. Activity of the Mos-MAPK pathway is required for tight spindle attachment to the cortex, proper chromosome separation and cleavage furrow closure. These functions are mediated by the activation of ApDia downstream of the Mos-MAPK pathway. ApDia is highly localized at the cleavage furrow where its activation most possibly drives F-actin formation during cleavage furrow closure.

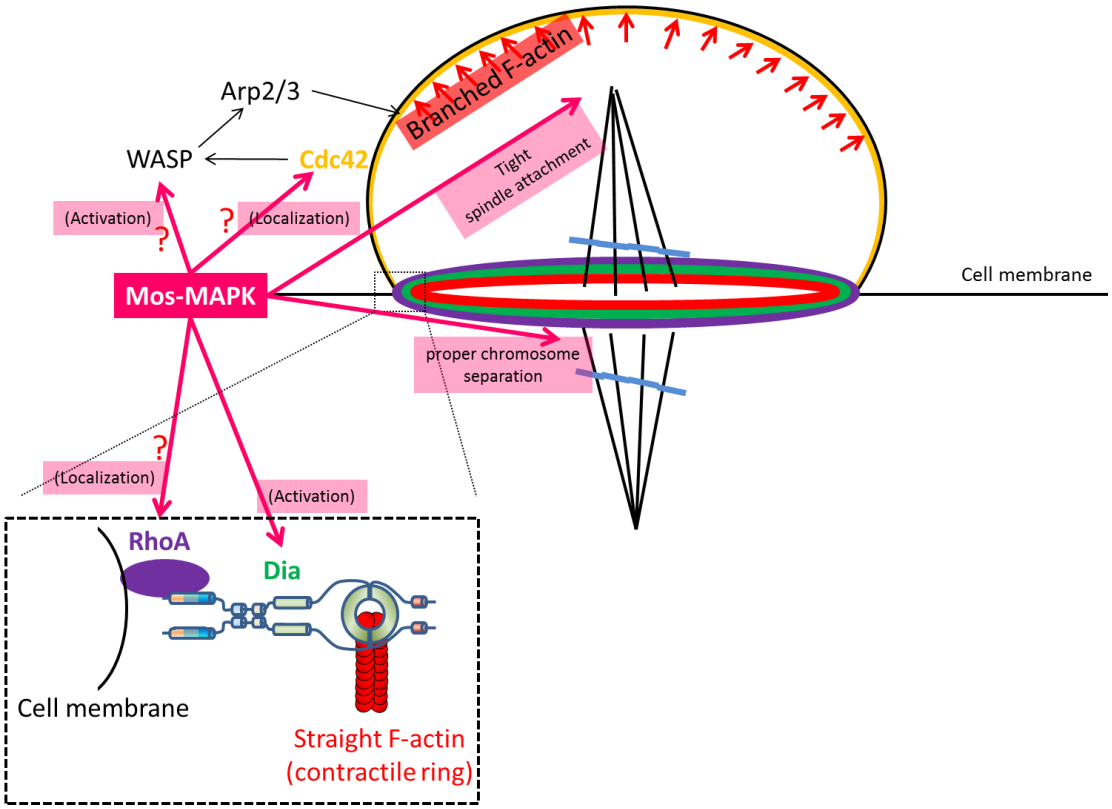

Fig. 5-2. Roles of Mos-MAPK pathway during PBE. In this study, I have shown that activity of the Mos-MAPK pathway is required for tight spindle attachment to cortex, proper chromosome separation and cleavage furrow closure during PBE, and the cleavage furrow closure is mediated by activation of Dia. Based on literature data and results of this study, it is plausible that the Mos- MAPK activity regulates localization of active-RhoA and active-Cdc42 and activation of Wasp during polar body emission.

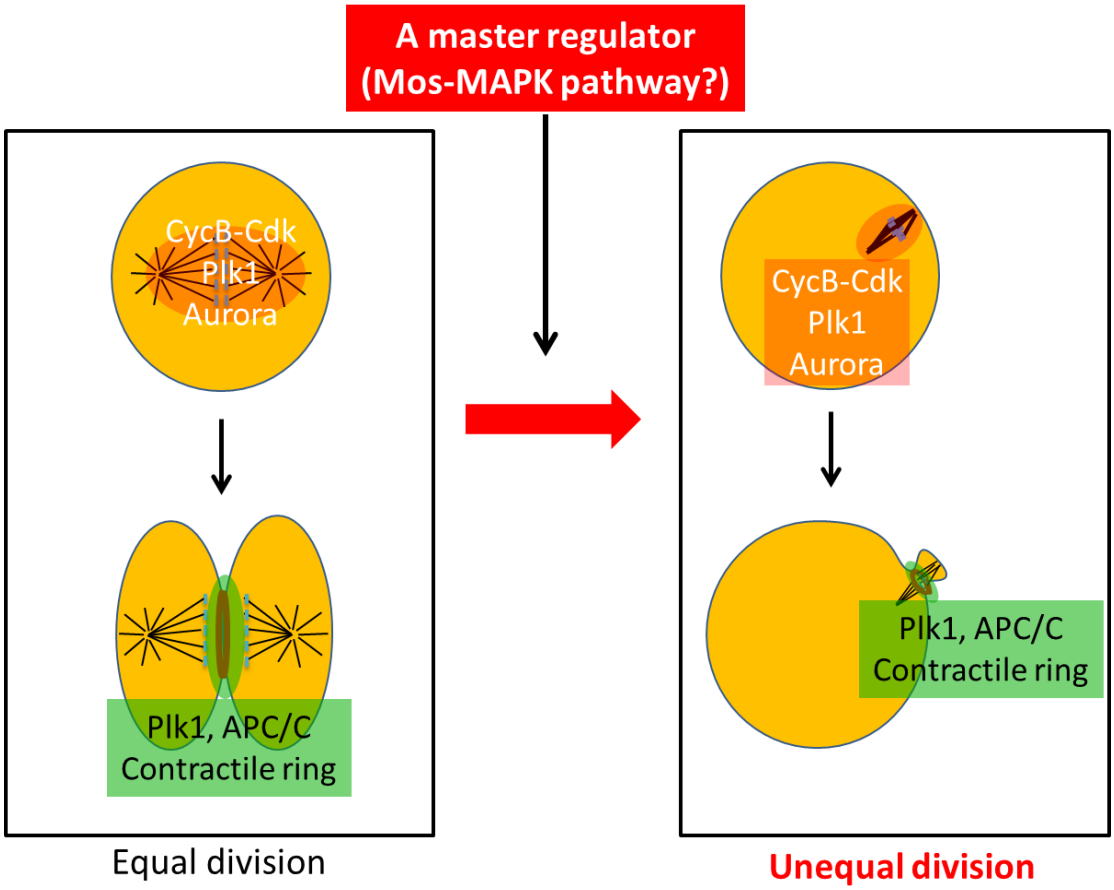

Fig. 5-3. What is the master regulator of unequal cell division? In both equal and unequal cell divisions the same cell cycle regulators and the same cytokinesis elements are functioning. The question is; what is the uppermost regulator that drives these cell division machineries to function under the cortex. Considering recent publications, can the Mos-MAPK pathway be a candidate for this role?

6. MATERIALS AND METHODS

Oocyte culture, extract preparation, and drug treatment

Fully grown immature *A. pectinifera* oocytes and oocyte extracts for western blotting were prepared as described previously (Okano-Uchida et al., 1998). Oocytes were incubated in 80% artificial sea water, Sealife (Marinetech, Japan) and maturation was induced by treatment with 1 µM 1-MeAde (Sigma). Diameters of oocytes (d_{oocyte}) and GV (d_{GV}) were measured; average diameters were, d_{oocyte} = 208.8 µm and d_{GV} = 85.0 µm (d_{oocyte}/d_{GV} = 0.41) in fully grown oocytes, and d_{oocyte} = 199.4 µm and d_{GV} = 72.2 µm (d_{oocyte}/d_{GV} = 0.36) in non-fully grown oocytes. To inhibit MEK activity, immature oocytes were treated with U0126 (Sigma). FH2 activity of formins was inhibited by treatment with 100 µM SMIFH2 (Calbiochem) 30 minutes after maturation induction.

Protein and mRNA preparation

ApDia was cloned from a cDNA library prepared from immature *A. pectinifera* oocytes. For the GST-ApDia-GBD and GST-ApDia-DAD peptides; amino acids 1–323 and 1004–1105 of ApDia were cloned into pGEX-4T-2, and bacterially expressed proteins were purified as described by the manufacturer (GE Healthcare). The GST-mDia-GBD (amino acids 1–300) was a gift from Prof. Hiroshi Itoh (Nara Institute of Science and Technology). mDia-GBD/DID was tagged with GFP and cloned into pET21a (Novagen) to prepare GFP-mDia-GBD/DID protein. To prepare mRNA, the GFP2 DNA sequence was obtained from Clontech, and full-length ApDia tagged with HA-GFP2 at the N-terminus was cloned into a modified pSP64 (Promega) which contained *Xenopus* globin 5`UTR and 3`UTR sequences. Cloning was done by In-Fusion

PCR cloning system (Clontech). Site-directed mutagenesis was performed with the QuikChange kit (Stratagene).. Plasmids were linearized with SmaI and mRNA was synthesized using the mMESSAGE mMACHINE SP6 kit (Invitrogen).

Microinjection and microscopy

Microinjection was performed as described previously (Kishimoto, 1986). For Mos experiments, immature oocytes were injected with 100 pg control oligonucleotide (AT*GCCT*T*GCGACACGGC) or 100 pg MosAS (CGGCT*GT*CGCAAGGCAT) (Tachibana et al., 2000) together with HiLyte-488-labeled tubulin (Cytoskeleton) and Alexa568-labeled histone H1 (Hara et al., 2012) and meiotic maturation was induced 30 minutes after injection. For inhibitor treatments, immature oocytes were injected with HiLyte-488-labeled tubulin and Alexa568-labeled histone H1 and meiotic maturation was induced 30 minutes after injection (U0126 was administered together with 1-MeAde but SMIFH2 was administered 30 min after 1-MeAde). To activate endogenous ApDia, immature oocytes were injected with 2.4 pg GST-ApDia-DAD, 10 pg GST-ApDia-GBD/DID or 10 pg GFP-mDia-GBD/DID proteins together with HiLyte-488-labeled tubulin and Alexa568-labeled histone H1, and then meiotic maturation was induced 30 minutes after injection. For mRNA injection experiments, immature oocytes were injected with 150 pg mRNA of HA-GFP2-ApDia, HA-GFP2-ApDia-fsDAD or HA-GFP2-ApDia-fsDAD-I699A together with rhodamine-labeled tubulin (Cytoskeleton), oocytes were incubated for 5 hours at 19 °C to allow proteins to be expressed, and then meiotic maturation was induced in the presence of DMSO or U0126. Live-cell imaging was performed with Olympus

Fluoview-1000 confocal microscope equipped with a 40X water immersion objective.10 to 24 Z-section images spanning a depth of 7 to 15 µm were captured approximately at 1 min intervals during oocyte maturation. Z-sections were then piled to represent single time points and movies were prepared with the piled images. All experiments were done at least 3 times with different animals.

Immunoblotting

Immunoblotting was performed as described previously (Okano-Uchida et al., 1998). Proteins were blotted to Immobilon-P membrane (Milipore) by semi-dry blotting. Membranes were blocked with 5% skimy milk (for MAPK and p90Rsk) or 2% Advanced blocking solution (GE Healthcare) (for HA tag) for 1 h at room temperature (RT). After 3 times washing with TBS-T (Tris-buffered saline + 0.05% Tween-20), antibodies were administered on membranes overnight at 4°C. Antibody dilutions were as follow; Anti-MAPK (Milipore) 1:500 in TBS-T, anti-p90Rsk 1:200 in TBS-T, anti-HA 1:1000 in Hikari-A solution (GE Healthcare). After 3 times washing with TBS-T, HRP conjugated anti-rabbit IgG (MAPK and p90Rsk) or anti-rat IgG (HA) secondary antibodies (1:5000 dilution each) were administered at RT for 1 h. After washing with TBS-T 3 times, detection was done with ECL western blotting substrate kit (GE Healthcare) for MAPK and p90Rsk or ECL Advance western blotting detection kit (GE Healthcare) for HA.

7. REFERENCES

Abe, Y., Okumura, E., Hosoya, T., Hirota, T. and Kishimoto, T. (2010). A single starfish Aurora kinase performs the combined functions of Aurora-A and Aurora-B in human cells. *J. Cell. Sci.* **123**, 3978–3988.

Amiel, A., Leclère, L., Robert, L., Chevalier, S. and Houliston, E. (2009). Conserved functions for Mos in eumetazoan oocyte maturation revealed by studies in a cnidarian. *Curr. Biol.* **19**, 305–311.

Azoury, J., Verlhac, M.-H. and Dumont, J. (2009). Actin filaments: key players in the control of asymmetric divisions in mouse oocytes. *Biol. Cell* **101**, 69–76.

Azoury, J., Lee, K. W., Georget, V., Hikal, P. and Verlhac, M.-H. (2011). Symmetry breaking in mouse oocytes requires transient F-actin meshwork destabilization. *Development* **138**, 2903–2908.

Barr, F. A. and Gruneberg, U. (2007). Cytokinesis: placing and making the final cut. *Cell* **131**, 847–860.

Bartolini, F., Moseley, J. B., Schmoranzer, J., Cassimeris, L., Goode, B. L. and Gundersen, G. G. (2008). The formin mDia2 stabilizes microtubules independently of its actin nucleation activity. *J. Cell Biol.* **181**, 523–536.

Bell, S. P. and Dutta, A. (2002). DNA replication in eukaryotic cells. *Annu. Rev. Biochem.* **71**, 333–374.

Bhatt, R. R. and Ferrell, J. E., Jr (1999). The protein kinase p90 rsk as an

essential mediator of cytostatic factor activity. *Science* **286**, 1362–1365.

Campellone, K. G. and Welch, M. D. (2010). A nucleator arms race: cellular control of actin assembly. *Nat. Rev. Mol. Cell Biol.* **11**, 237–251.

Chaigne, A., Campillo, C., Gov, N. S., Voituriez, R., Azoury, J., Umaña-Diaz, C., Almonacid, M., Queguiner, I., Nassoy, P., Sykes, C., et al. (2013). A soft cortex is essential for asymmetric spindle positioning in mouse oocytes. *Nat Cell Biol* **advance online publication**,.

Cheeseman, I. M. and Desai, A. (2008). Molecular architecture of the kinetochore–microtubule interface. *Nat Rev Mol Cell Biol* **9**, 33–46.

Chen, H., Kuo, C.-C., Kang, H., Howell, A. S., Zyla, T. R., Jin, M. and Lew, D. J. (2012). Cdc42p regulation of the yeast formin Bni1p mediated by the effector Gic2p. *Mol. Biol. Cell* **23**, 3814–3826.

Cheng, L., Zhang, J., Ahmad, S., Rozier, L., Yu, H., Deng, H. and Mao, Y. (2011). Aurora B regulates formin mDia3 in achieving metaphase chromosome alignment. *Dev. Cell* **20**, 342–352.

Chesarone, M. A., DuPage, A. G. and Goode, B. L. (2010). Unleashing formins to remodel the actin and microtubule cytoskeletons. *Nat. Rev. Mol. Cell Biol.* **11**, 62–74.

Choi, T., Fukasawa, K., Zhou, R., Tessarollo, L., Borror, K., Resau, J. and Vande Woude, G. F. (1996). The Mos/mitogen-activated protein kinase (MAPK) pathway regulates the size and degradation of the first polar

body in maturing mouse oocytes. *Proc. Natl. Acad. Sci. U.S.A.* **93**, 7032–7035.

Cohen-Fix, O. and Koshland, D. (1997). The metaphase-to-anaphase transition: avoiding a mid-life crisis. *Curr. Opin. Cell Biol.* **9**, 800–806.

Comings, D. E. and Riggs, A. D. (1971). Molecular mechanisms of chromosome pairing, folding and function. *Nature* **233**, 48–50.

Compton, D. A. (2000). Spindle assembly in animal cells. *Annu. Rev. Biochem.* **69**, 95–114.

Cooper, S. (1979). A unifying model for the G1 period in prokaryotes and eukaryotes. *Nature* **280**, 17–19.

Cowan, C. (2007). Ran and Rac in mouse eggs: cortical polarity and spindle positioning. *Dev. Cell* **12**, 174–176.

Cromie, G. A. and Smith, G. R. (2007). Branching out: meiotic recombination and its regulation. *Trends Cell Biol.* **17**, 448–455.

Deng, M., Suraneni, P., Schultz, R. M. and Li, R. (2007). The Ran GTPase mediates chromatin signaling to control cortical polarity during polar body extrusion in mouse oocytes. *Dev. Cell* **12**, 301–308.

Dorée, M. and Hunt, T. (2002). From Cdc2 to Cdk1: when did the cell cycle kinase join its cyclin partner? *J. Cell. Sci.* **115**, 2461–2464.

Doxsey, S. (2001). Re-evaluating centrosome function. *Nat. Rev. Mol. Cell Biol.* **2**, 688–698.

Dumont, J., Million, K., Sunderland, K., Rassinier, P., Lim, H., Leader, B. and Verlhac, M.-H. (2007). Formin-2 is required for spindle migration and for the late steps of cytokinesis in mouse oocytes. *Dev. Biol.* **301**, 254–265.

Duncan, F. E., Moss, S. B., Schultz, R. M. and Williams, C. J. (2005). PAR-3 defines a central subdomain of the cortical actin cap in mouse eggs. *Dev. Biol.* **280**, 38–47.

Dupré, A., Jessus, C., Ozon, R. and Haccard, O. (2002). Mos is not required for the initiation of meiotic maturation in Xenopus oocytes. *EMBO J.* **21**, 4026–4036.

Dupré, A., Haccard, O. and Jessus, C. (2011). Mos in the oocyte: how to use MAPK independently of growth factors and transcription to control meiotic divisions. *J Signal Transduct* **2011**, 350412.

Eckerdt, F. and Strebhardt, K. (2006). Polo-like kinase 1: target and regulator of anaphase-promoting complex/cyclosome-dependent proteolysis. *Cancer Res.* **66**, 6895–6898.

Evangelista, M., Blundell, K., Longtine, M. S., Chow, C. J., Adames, N., Pringle, J. R., Peter, M. and Boone, C. (1997). Bni1p, a yeast formin linking cdc42p and the actin cytoskeleton during polarized morphogenesis. *Science* **276**, 118–122.

Evans, J. P. and Robinson, D. N. (2011). The spatial and mechanical challenges of female meiosis. *Mol. Reprod. Dev.* **78**, 769–777.

Fededa, J. P. and Gerlich, D. W. (2012a). Molecular control of animal cell cytokinesis. *Nat. Cell Biol.* **14**, 440–447.

Fededa, J. P. and Gerlich, D. W. (2012b). Molecular control of animal cell cytokinesis. *Nat. Cell Biol.* **14**, 440–447.

Field, C., Li, R. and Oegema, K. (1999). Cytokinesis in eukaryotes: a mechanistic comparison. *Curr. Opin. Cell Biol.* **11**, 68–80.

Gao, L., Liu, W. and Bretscher, A. (2010). The yeast formin Bnr1p has two localization regions that show spatially and temporally distinct association with septin structures. *Mol. Biol. Cell* **21**, 1253–1262.

Gard, D. L. (1992). Microtubule organization during maturation of Xenopus oocytes: assembly and rotation of the meiotic spindles. *Dev. Biol.* **151**, 516–530.

Gould, C. J., Maiti, S., Michelot, A., Graziano, B. R., Blanchoin, L. and Goode, B. L. (2011). The formin DAD domain plays dual roles in autoinhibition and actin nucleation. *Curr. Biol.* **21**, 384–390.

Gross, S. D., Schwab, M. S., Lewellyn, A. L. and Maller, J. L. (1999). Induction of metaphase arrest in cleaving Xenopus embryos by the protein kinase p90Rsk. *Science* **286**, 1365–1367.

Gross, S. D., Schwab, M. S., Taieb, F. E., Lewellyn, A. L., Qian, Y. W. and Maller, J. L. (2000). The critical role of the MAP kinase pathway in meiosis II in Xenopus oocytes is mediated by p90(Rsk). *Curr. Biol.* **10**, 430–438.

Haccard, O., Sarcevic, B., Lewellyn, A., Hartley, R., Roy, L., Izumi, T., Erikson, E. and Maller, J. L. (1993). Induction of metaphase arrest in cleaving Xenopus embryos by MAP kinase. *Science* **262**, 1262–1265.

Halet, G. and Carroll, J. (2007). Rac activity is polarized and regulates meiotic spindle stability and anchoring in mammalian oocytes. *Dev. Cell* **12**, 309–317.

Hara, M., Mori, M., Wada, T., Tachibana, K. and Kishimoto, T. (2009). Start of the embryonic cell cycle is dually locked in unfertilized starfish eggs. *Development* **136**, 1687–1696.

Hara, M., Abe, Y., Tanaka, T., Yamamoto, T., Okumura, E. and Kishimoto, T. (2012). Greatwall kinase and cyclin B-Cdk1 are both critical constituents of M-phase-promoting factor. *Nat Commun* **3**, 1059.

Hartwell, L. H. and Weinert, T. A. (1989). Checkpoints: controls that ensure the order of cell cycle events. *Science* **246**, 629–634.

Hawkins, N. and Garriga, G. (1998). Asymmetric cell division: from A to Z. *Genes Dev.* **12**, 3625–3638.

Horvitz, H. R. and Herskowitz, I. (1992). Mechanisms of asymmetric cell division: two Bs or not two Bs, that is the question. *Cell* **68**, 237–255.

Inoue, D., Ohe, M., Kanemori, Y., Nobui, T. and Sagata, N. (2007). A direct link of the Mos-MAPK pathway to Erp1/Emi2 in meiotic arrest of Xenopus laevis eggs. *Nature* **446**, 1100–1104.

Ishizaki, T., Morishima, Y., Okamoto, M., Furuyashiki, T., Kato, T. and

Narumiya, S. (2001). Coordination of microtubules and the actin cytoskeleton by the Rho effector mDia1. *Nat. Cell Biol.* **3**, 8–14.

John, P. C., Mews, M. and Moore, R. (2001). Cyclin/Cdk complexes: their involvement in cell cycle progression and mitotic division. *Protoplasma* **216**, 119–142.

Johnson, A. D., Richardson, E., Bachvarova, R. F. and Crother, B. I. (2011). Evolution of the germ line-soma relationship in vertebrate embryos. *Reproduction* **141**, 291–300.

Kaltschmidt, J. A. and Brand, A. H. (2002). Asymmetric cell division: microtubule dynamics and spindle asymmetry. *J. Cell. Sci.* **115**, 2257–2264.

Kerkhoff, E. (2011). Actin dynamics at intracellular membranes: the Spir/formin nucleator complex. *Eur. J. Cell Biol.* **90**, 922–925.

Kerkhoff, E., Simpson, J. C., Leberfinger, C. B., Otto, I. M., Doerks, T., Bork, P., Rapp, U. R., Raabe, T. and Pepperkok, R. (2001). The Spir actin organizers are involved in vesicle transport processes. *Curr. Biol.* **11**, 1963–1968.

Kishimoto, T. (1986). Microinjection and cytoplasmic transfer in starfish oocytes. *Methods Cell Biol.* **27**, 379–394.

Kishimoto, T. (1998). Cell cycle arrest and release in starfish oocytes and eggs. *Semin. Cell Dev. Biol.* **9**, 549–557.

Kishimoto, T. (2003). Cell-cycle control during meiotic maturation. *Curr. Opin.*

Cell Biol. **15**, 654–663.

Kosako, H., Gotoh, Y. and Nishida, E. (1994). Mitogen-activated protein kinase kinase is required for the mos-induced metaphase arrest. *J. Biol. Chem.* **269**, 28354–28358.

Kumano, M., Carroll, D. J., Denu, J. M. and Foltz, K. R. (2001). Calcium-mediated inactivation of the MAP kinase pathway in sea urchin eggs at fertilization. *Dev. Biol.* **236**, 244–257.

Laskey, R. A., Fairman, M. P. and Blow, J. J. (1989). S phase of the cell cycle. *Science* **246**, 609–614.

Lebensohn, A. M. and Kirschner, M. W. (2009). Activation of the WAVE complex by coincident signals controls actin assembly. *Mol. Cell* **36**, 512–524.

Lee, J., Miyano, T. and Moor, R. M. (2000). Localisation of phosphorylated MAP kinase during the transition from meiosis I to meiosis II in pig oocytes. *Zygote* **8**, 119–125.

Lee, S.-E., Kim, J.-H. and Kim, N.-H. (2007). Inactivation of MAPK affects centrosome assembly, but not actin filament assembly, in mouse oocytes maturing in vitro. *Mol. Reprod. Dev.* **74**, 904–911.

Lee, I.-J., Coffman, V. C. and Wu, J.-Q. (2012). Contractile-ring assembly in fission yeast cytokinesis: Recent advances and new perspectives. *Cytoskeleton (Hoboken)* **69**, 751–763.

Lei, M. and Tye, B. K. (2001). Initiating DNA synthesis: from recruiting to

activating the MCM complex. *J. Cell. Sci.* **114**, 1447–1454.

Lénárt, P., Rabut, G., Daigle, N., Hand, A. R., Terasaki, M. and Ellenberg, J. (2003). Nuclear envelope breakdown in starfish oocytes proceeds by partial NPC disassembly followed by a rapidly spreading fenestration of nuclear membranes. *J. Cell Biol.* **160**, 1055–1068.

Li, R. and Albertini, D. F. (2013). The road to maturation: somatic cell interaction and self-organization of the mammalian oocyte. *Nat. Rev. Mol. Cell Biol.* **14**, 141–152.

Li, F. and Higgs, H. N. (2003). The mouse Formin mDia1 is a potent actin nucleation factor regulated by autoinhibition. *Curr. Biol.* **13**, 1335–1340.

Lu, M. S. and Johnston, C. A. (2013). Molecular pathways regulating mitotic spindle orientation in animal cells. *Development* **140**, 1843–1856.

Maddox, A. S., Azoury, J. and Dumont, J. (2012). Polar body cytokinesis. *Cytoskeleton (Hoboken)* **69**, 855–868.

Maguire, M. P. (1990). Sister chromatid cohesiveness: vital function, obscure mechanism. *Biochem. Cell Biol.* **68**, 1231–1242.

Maller, J. L. (1985). Regulation of amphibian oocyte maturation. *Cell Differ.* **16**, 211–221.

Malumbres, M. and Barbacid, M. (2005). Mammalian cyclin-dependent kinases. *Trends Biochem. Sci.* **30**, 630–641.

Mao, Y. (2011). FORMIN a link between kinetochores and microtubule ends.

Trends Cell Biol. **21**, 625–629.

Masui, Y. and Markert, C. L. (1971). Cytoplasmic control of nuclear behavior during meiotic maturation of frog oocytes. *J. Exp. Zool.* **177**, 129–145.

Matsumura, F., Yamakita, Y. and Yamashiro, S. (2011). Myosin light chain kinases and phosphatase in mitosis and cytokinesis. *Arch. Biochem. Biophys.* **510**, 76–82.

Matsuura, R. and Chiba, K. (2004). Unequal cell division regulated by the contents of germinal vesicles. *Dev. Biol.* **273**, 76–86.

McCarthy, E. K. and Goldstein, B. (2006). Asymmetric spindle positioning. *Curr. Opin. Cell Biol.* **18**, 79–85.

McNally, F. J. (2013). Mechanisms of spindle positioning. *J. Cell Biol.* **200**, 131–140.

Mendoza, M. C., Er, E. E., Zhang, W., Ballif, B. A., Elliott, H. L., Danuser, G. and Blenis, J. (2011). ERK-MAPK drives lamellipodia protrusion by activating the WAVE2 regulatory complex. *Mol. Cell* **41**, 661–671.

Miller, A. L. and Bement, W. M. (2009). Cell division: the need for speed. *Curr. Biol.* **19**, R1071–1073.

Mitchison, T. J. and Salmon, E. D. (2001). Mitosis: a history of division. *Nat. Cell Biol.* **3**, E17–21.

Mori, M., Hara, M., Tachibana, K. and Kishimoto, T. (2006). p90Rsk is required for G1 phase arrest in unfertilized starfish eggs. *Development*

133, 1823–1830.

Mori, M., Monnier, N., Daigle, N., Bathe, M., Ellenberg, J. and Lénárt, P. (2011). Intracellular transport by an anchored homogeneously contracting F-actin meshwork. *Curr. Biol.* **21**, 606–611.

Murray, A. (1994). Cell cycle checkpoints. *Curr. Opin. Cell Biol.* **6**, 872–876.

Murray, A. and Hunt, T. (1994). The cell cycle: An introduction, by Andrew Murray and Tim Hunt, W.H. Freeman&co., New York, distributed by oxford university press, 1993, 251pp, $22.95. *Molecular Reproduction and Development* **39**, 247–247.

Nance, J. (2005). PAR proteins and the establishment of cell polarity during C. elegans development. *Bioessays* **27**, 126–135.

Nasmyth, K. (2005). How do so few control so many? *Cell* **120**, 739–746.

Nezami, A., Poy, F., Toms, A., Zheng, W. and Eck, M. J. (2010). Crystal structure of a complex between amino and carboxy terminal fragments of mDia1: insights into autoinhibition of diaphanous-related formins. *PLoS ONE* **5**,.

Nigg, E. A. (1995). Cyclin-dependent protein kinases: key regulators of the eukaryotic cell cycle. *Bioessays* **17**, 471–480.

Nigg, E. A. (1998). Polo-like kinases: positive regulators of cell division from start to finish. *Curr. Opin. Cell Biol.* **10**, 776–783.

Nishiyama, T., Ohsumi, K. and Kishimoto, T. (2007). Phosphorylation of

Erp1 by p90rsk is required for cytostatic factor arrest in Xenopus laevis eggs. *Nature* **446**, 1096–1099.

Nurse, P. (1994). Ordering S phase and M phase in the cell cycle. *Cell* **79**, 547–550.

Okano-Uchida, T., Sekiai, T., Lee, K., Okumura, E., Tachibana, K. and Kishimoto, T. (1998). In vivo regulation of cyclin A/Cdc2 and cyclin B/Cdc2 through meiotic and early cleavage cycles in starfish. *Dev. Biol.* **197**, 39–53.

Okano-Uchida, T., Okumura, E., Iwashita, M., Yoshida, H., Tachibana, K. and Kishimoto, T. (2003). Distinct regulators for Plk1 activation in starfish meiotic and early embryonic cycles. *EMBO J.* **22**, 5633–5642.

Otomo, T., Tomchick, D. R., Otomo, C., Machius, M. and Rosen, M. K. (2010). Crystal structure of the Formin mDia1 in autoinhibited conformation. *PLoS ONE* **5**,.

Palazzo, A. F., Cook, T. A., Alberts, A. S. and Gundersen, G. G. (2001). mDia mediates Rho-regulated formation and orientation of stable microtubules. *Nat. Cell Biol.* **3**, 723–729.

Pardee, A. B. (1989). G1 events and regulation of cell proliferation. *Science* **246**, 603–608.

Paules, R. S., Buccione, R., Moschel, R. C., Vande Woude, G. F. and Eppig, J. J. (1989). Mouse Mos protooncogene product is present and functions during oogenesis. *Proc. Natl. Acad. Sci. U.S.A.* **86**, 5395–

5399.

Paweletz, N. (2001). Walther Flemming: pioneer of mitosis research. *Nat Rev Mol Cell Biol* **2**, 72–75.

Peters, J.-M. (2006). The anaphase promoting complex/cyclosome: a machine designed to destroy. *Nat. Rev. Mol. Cell Biol.* **7**, 644–656.

Petronczki, M., Lénárt, P. and Peters, J.-M. (2008). Polo on the Rise-from Mitotic Entry to Cytokinesis with Plk1. *Dev. Cell* **14**, 646–659.

Pfender, S., Kuznetsov, V., Pleiser, S., Kerkhoff, E. and Schuh, M. (2011). Spire-type actin nucleators cooperate with Formin-2 to drive asymmetric oocyte division. *Curr. Biol.* **21**, 955–960.

Phadnis, N., Hyppa, R. W. and Smith, G. R. (2011). New and old ways to control meiotic recombination. *Trends Genet.* **27**, 411–421.

Pines, J. (1999). Four-dimensional control of the cell cycle. *Nat. Cell Biol.* **1**, E73–79.

Rasmussen, S. W. and Holm, P. B. (1980). Mechanics of meiosis. *Hereditas* **93**, 187–216.

Riley, R. and Flavell, R. B. (1977). A first view of the meiotic process. *Philos. Trans. R. Soc. Lond., B, Biol. Sci.* **277**, 191–199.

Rizvi, S. A., Neidt, E. M., Cui, J., Feiger, Z., Skau, C. T., Gardel, M. L., Kozmin, S. A. and Kovar, D. R. (2009). Identification and characterization of a small molecule inhibitor of formin-mediated actin

assembly. *Chem. Biol.* **16**, 1158–1168.

Rouiller, I., Xu, X.-P., Amann, K. J., Egile, C., Nickell, S., Nicastro, D., Li, R., Pollard, T. D., Volkmann, N. and Hanein, D. (2008). The structural basis of actin filament branching by the Arp2/3 complex. *J. Cell Biol.* **180**, 887–895.

Sagata, N. (1996). Meiotic metaphase arrest in animal oocytes: its mechanisms and biological significance. *Trends Cell Biol.* **6**, 22–28.

Sagata, N., Watanabe, N., Vande Woude, G. F. and Ikawa, Y. (1989). The c-mos proto-oncogene product is a cytostatic factor responsible for meiotic arrest in vertebrate eggs. *Nature* **342**, 512–518.

Sagot, I., Klee, S. K. and Pellman, D. (2002). Yeast formins regulate cell polarity by controlling the assembly of actin cables. *Nat. Cell Biol.* **4**, 42–50.

Schiel, J. A. and Prekeris, R. (2013). Membrane dynamics during cytokinesis. *Curr. Opin. Cell Biol.* **25**, 92–98.

Swan, K. A., Severson, A. F., Carter, J. C., Martin, P. R., Schnabel, H., Schnabel, R. and Bowerman, B. (1998). cyk-1: a C. elegans FH gene required for a late step in embryonic cytokinesis. *J Cell Sci* **111**, 2017–2027.

Tachibana, K., Machida, T., Nomura, Y. and Kishimoto, T. (1997). MAP kinase links the fertilization signal transduction pathway to the G1/S-phase transition in starfish eggs. *EMBO J.* **16**, 4333–4339.

Tachibana, K., Tanaka, D., Isobe, T. and Kishimoto, T. (2000). c-Mos forces the mitotic cell cycle to undergo meiosis II to produce haploid gametes. *Proc. Natl. Acad. Sci. U.S.A.* **97**, 14301–14306.

Tachibana, K., Mori, M., Matsuhira, T., Karino, T., Inagaki, T., Nagayama, A., Nishiyama, A., Hara, M. and Kishimoto, T. (2010). Initiation of DNA replication after fertilization is regulated by p90Rsk at pre-RC/pre-IC transition in starfish eggs. *Proc. Natl. Acad. Sci. U.S.A.* **107**, 5006–5011.

Tatsumoto, T., Xie, X., Blumenthal, R., Okamoto, I. and Miki, T. (1999). Human ECT2 is an exchange factor for Rho GTPases, phosphorylated in G2/M phases, and involved in cytokinesis. *J. Cell Biol.* **147**, 921–928.

Taylor, S. and Peters, J.-M. (2008). Polo and Aurora kinases: lessons derived from chemical biology. *Curr. Opin. Cell Biol.* **20**, 77–84.

Tomasevic, N., Jia, Z., Russell, A., Fujii, T., Hartman, J. J., Clancy, S., Wang, M., Beraud, C., Wood, K. W. and Sakowicz, R. (2007). Differential regulation of WASP and N-WASP by Cdc42, Rac1, Nck, and PI(4,5)P2. *Biochemistry* **46**, 3494–3502.

Tong, C., Fan, H. Y., Chen, D. Y., Song, X. F., Schatten, H. and Sun, Q. Y. (2003). Effects of MEK inhibitor U0126 on meiotic progression in mouse oocytes: microtuble organization, asymmetric division and metaphase II arrest. *Cell Res.* **13**, 375–383.

Verlhac, M.-H. and Dumont, J. (2008). Interactions between chromosomes, microfilaments and microtubules revealed by the study of small

GTPases in a big cell, the vertebrate oocyte. *Mol. Cell. Endocrinol.* **282**, 12–17.

Verlhac, M. H., Lefebvre, C., Guillaud, P., Rassinier, P. and Maro, B. (2000). Asymmetric division in mouse oocytes: with or without Mos. *Curr. Biol.* **10**, 1303–1306.

Vinot, S., Le, T., Maro, B. and Louvet-Vallée, S. (2004). Two PAR6 proteins become asymmetrically localized during establishment of polarity in mouse oocytes. *Curr. Biol.* **14**, 520–525.

Vizcarra, C. L., Kreutz, B., Rodal, A. A., Toms, A. V., Lu, J., Zheng, W., Quinlan, M. E. and Eck, M. J. (2011). Structure and function of the interacting domains of Spire and Fmn-family formins. *Proc. Natl. Acad. Sci. U.S.A.* **108**, 11884–11889.

Vodermaier, H. C. (2004). APC/C and SCF: controlling each other and the cell cycle. *Curr. Biol.* **14**, R787–796.

Watanabe, S., Ando, Y., Yasuda, S., Hosoya, H., Watanabe, N., Ishizaki, T. and Narumiya, S. (2008). mDia2 induces the actin scaffold for the contractile ring and stabilizes its position during cytokinesis in NIH 3T3 cells. *Mol. Biol. Cell* **19**, 2328–2338.

Watanabe, S., Okawa, K., Miki, T., Sakamoto, S., Morinaga, T., Segawa, K., Arakawa, T., Kinoshita, M., Ishizaki, T. and Narumiya, S. (2010). Rho and anillin-dependent control of mDia2 localization and function in cytokinesis. *Mol. Biol. Cell* **21**, 3193–3204.

Weiss, E. L. (2012). Mitotic exit and separation of mother and daughter cells. *Genetics* **192**, 1165–1202.

Yanowitz, J. (2010). Meiosis: making a break for it. *Curr. Opin. Cell Biol.* **22**, 744–751.

Yi, K. and Li, R. (2012). Actin cytoskeleton in cell polarity and asymmetric division during mouse oocyte maturation. *Cytoskeleton (Hoboken)* **69**, 727–737.

Yu, L.-Z., Xiong, B., Gao, W.-X., Wang, C.-M., Zhong, Z.-S., Huo, L.-J., Wang, Q., Hou, Y., Liu, K., Liu, X. J., et al. (2007). MEK1/2 regulates microtubule organization, spindle pole tethering and asymmetric division during mouse oocyte meiotic maturation. *Cell Cycle* **6**, 330–338.

Yu, J. H., Crevenna, A. H., Bettenbühl, M., Freisinger, T. and Wedlich-Söldner, R. (2011). Cortical actin dynamics driven by formins and myosin V. *J. Cell. Sci.* **124**, 1533–1541.

Zhang, X., Ma, C., Miller, A. L., Katbi, H. A., Bement, W. M. and Liu, X. J. (2008). Polar body emission requires a RhoA contractile ring and Cdc42-mediated membrane protrusion. *Dev. Cell* **15**, 386–400.

8. ACKNOWLEDGEMENTS

First of all, I would like to state my deepest gratitude to Professor Kishimoto Takeo, for giving me the opportunity to join his lab at the very beginning, for supporting me during my life in Japan not only in the research related matters but also in all aspects, and for strongly enhancing my way to a good postdoctoral position by believing in my passion for a good academic career. I would like to thank Dr Tachibana Kazunori, Dr Okumura Eiichi, Dr Mori Masashi, Dr Hara Masatoshi, Dr Hiraoka Daisuke and all the members of Kishimoto-Tachibana laboratory for helping me at several steps of my studies. I would like to state my thankfulness to Tada Yumiko for kindly helping me in all the complicated Japanese procedures.

I would like to thank the Ministry of Education, Culture, Sports, Science and Technology of Japan for providing me the opportunity to study in Japan. I thank Hiroshi Itoh for supplying the GST-GBD fragment of mDia and Eiichi Okumura for supplying Alexa-568-labeled histone H1.

Lastly but most importantly, I would like to state my appreciation to my family and my wife for supporting me emotionally and physically against all the hardships that I have encountered during my studies.

In Turkish; Son olarak, doktora çalışmalarım süresince, ayrılığın zorluklarına katlanma fedakarlığını göstermenin yanısıra, maddi ve manevi desteklerini hiç bir zaman esirgemeyen sevgili anneme, babama ve kardeşlerime en derin sevgi ve saygılarım ile teşekkür ederim. Doktora çalışmalarımın en yoğun olduğu dönemlerde her zaman yanıbaşımda bana destek olan, sıcak gülümsemesi ile tüm sıkıntılarımı gideren hayat arkadaşım sevgili eşime ise kalbimin en derinlerinden teşekkür ederim,